MOLECULAR AND CELLULAR BIOLOGY, June 2008, p. 3952–3966 Vol. 28, No. 12
0270-7306/08/$08.00+0 doi:10.1128/MCB.01439-07

A Novel Protein, Luman/CREB3 Reruitment Factor, Inhibits Luman Activation of the Unfolded Protein Response▽

Timothy E. Audas, Yu Li, Genqing Liang, and Rui Lu*

Department of Molecular and Cellular Biology, University of Guelph, Guelph, Ontario, Canada N1G 2W1

Received 10 August 2007/Returned for modification 4 October 2007/Accepted 25 March 2008

Luman/CREB3 (also called LZIP) is an endoplasmic reticulum (ER)-bound cellular transcription factor. It has been implicated in the mammalian unfolded protein response (UPR), as well as herpes simplex virus reactivation from latency in sensory neurons. Here, we report the identification of a novel Luman recruitment factor (LRF). Like Luman, LRF is a UPR-responsive basic-region leucine zipper protein that is prone to proteasomal degradation. Being a highly unstable protein, LRF interacts with Luman through the leucine zipper region and promotes Luman degradation. LRF was found to recruit the nuclear form of Luman to discrete nuclear foci, which overlap with the nuclear receptor coactivator GRIP1 bodies, and repress the transactivation activity of Luman. Compared to $LRF^{+/+}$ mouse embryonic fibroblast (MEF) cells, the levels of CHOP, EDEM, and Herp were elevated in $LRF^{-/-}$ MEF cells. We propose that LRF is a negative regulator of the UPR. For Luman, it may represent another level of regulation following Luman proteolytic cleavage on the ER and nuclear translocation. In addition to inducing rapid Luman turnover, LRF may repress the transactivation potential of Luman by sequestering it in the LRF nuclear bodies away from key cofactors (such as HCF-1) that are required for transcriptional activation.

The endoplasmic reticulum (ER) stress response (or unfolded protein response [UPR]) is a series of well-orchestrated cellular events to restore homeostasis in the perturbed ER. During the UPR, ER-resident molecular chaperones and foldases are induced, and translation is attenuated to reduce the load on the ER (reviewed in references 2, 49, 51, 67, 84, and 88). Unfolded proteins can also be targeted by ubiquitination for degradation by the proteasome, which is termed ER-associated degradation (ERAD) (35, 60, 70). Apoptosis occurs when all of these remedies have failed (16, 48, 63, 64). Current studies of the UPR mechanism in mammalian cells have identified three signaling arms represented by three ER membrane-bound proteins, PERK (PKR-like ER kinase) (14–18), ATF6α/β (19, 20, 75, 76, 92, 93), and IRE1 (6, 39, 78, 91). The activation of PERK by ER stress leads to global translational repression but selective activation of ATF4, whose downstream targets include metabolic genes and apoptosis-related CHOP (14, 26, 41, 55, 66, 80). ATF6 is an ER membrane-bound basic-region leucine zipper (bZIP) transcription factor that is activated by the regulated intramembrane proteolysis (RIP) mechanism (5). When ATF6 cleavage is triggered by ER stress (23, 87, 92, 93), the N terminus that encodes the transcription activation domain and the bZIP region translocates to the nucleus to activate downstream genes, such as ER chaperone BiP/GRP78 and GRP94, through the ER stress response element (ERSE) (65, 68, 82, 89, 92, 93). Activated IRE1 initiates spliceosome-independent alternative splicing of XBP1u mRNA, resulting in a potent bZIP transcription factor XBP1s (6, 39, 59, 69, 91). Like ATF6, XBP1s activates ER chaperone genes via an ERSE (91), but it also activates transcription through another *cis*-acting element, unfolded protein response element (UPRE) (82, 90). The known candidate genes potentially regulated by the UPRE enhancer include HRD1 (29), Derlins (56), and EDEM (ER degradation-enhancing α-mannosidase-like protein) (50, 90), all of which are believed to play a role in ERAD. Recent data suggest that ATF6 is also essential for ERAD (85, 86) as ATF6 can bind and activate transcription from the UPRE as a heterodimer with XBP1 (86).

Luman/CREB3 (44) (also called LZIP [13]) is the primary member of the CREB3 family. All CREB3 family members appear to play a role in the UPR. Currently, there are four known family members in addition to Luman, including CREB-H/CREB3-like 1 (CREB3L1) (8, 58), BBF2H7/CREB3L2 (73), OASIS/CREB3L3 (24), and CREB4/AIbZIP/Atce1/Tisp40/CREB3L4 (7, 53, 61, 71, 72). Besides the well-conserved bZIP region, they all share one unique structural motif—a hydrophobic ER-transmembrane domain C-terminal to the bZIP region. Under ER stress, these CREB3 proteins are thought to be cleaved by the same regulated intramembrane proteolysis mechanism as ATF6, translocating into the nucleus and activating downstream target genes (33, 40, 52, 53, 62, 72). They bind to various enhancer elements commonly found in the promoter region of UPR-related genes. All CREB3 proteins can activate transcription from CRE and UPRE (8, 11, 21, 33, 34, 44, 53, 57). In addition, CREB-H/CREB3L1 and OASIS/CREB3L3 bind box B and ERSE sequences (8, 33), while Luman and CREB-H/CREB3L1 also bind ERSE-II (8, 40).

Luman (44) was originally identified through its association with herpes simplex virus-related host cell factor 1 (HCF-1) (36, 83). The mode of interaction between Luman and HCF-1 is mimicked by the herpes simplex virus type 1 protein VP16, which has led to the hypothesis that Luman may play a role in viral reactivation from latency (13, 42, 45). Recently, the ERAD-related protein Herp (homocysteine-induced ER pro-

* Corresponding author. Mailing address: Department of Molecular and Cellular Biology, University of Guelph, Guelph, ON, Canada N1G 2W1. Phone: (519) 824-4120, ext. 56247. Fax: (519) 837-2075. E-mail: rlu@uoguelph.ca.

▽ Published ahead of print on 7 April 2008.

tein) (32) or Mif1 (79) has been found to be a direct downstream target of Luman (40). Luman induces cellular Herp expression during the UPR via transactivation of an ERSE-II enhancer element. Luman can also induce another ERAD protein, EDEM, likely through a UPRE-like element found in its promoter (11). We have thus proposed that Luman may be a cross talk point between different signaling pathways of UPR and that Luman plays a unique role in ERAD that is fundamental to the herpes simplex virus lytic/latent replication cycle (40). Recent data have also implicated Luman in human immunodeficiency virus replication (3) and monocyte cell migration (25).

To investigate the cellular role of Luman and to identify cellular proteins that regulate its activation, we sought to identify cellular binding proteins of Luman using a yeast two-hybrid system. In this paper we report the discovery of a novel cellular protein, termed Luman/CREB3 recruitment factor (LRF). LRF is induced by ER stress and appears to be a negative regulator of the UPR. We found that LRF recruited the nuclear Luman protein to discrete foci in the nucleus and repressed Luman-mediated activation of UPRE-containing promoters.

MATERIALS AND METHODS

Yeast two-hybrid screening and isolation of LRF cDNA clone. The bait plasmid pGBKT7-LubZIP was constructed by PCR amplification from the plasmid pFLAG-Luman (also called pcLuman) (44). The cDNA sequence coding for the leucine zipper domain of Luman (amino acids [aa] 162 to 228) was inserted into the pGBKT7 vector (Clontech) between the EcoRI-SalI sites. A pretransformed human fetal brain yeast two-hybrid library (MatchMakerIII; Clontech) was screened according to the manufacturer's instructions. Transformants were spread on a synthetic minimal dropout medium (0.67% [wt/vol] yeast nitrogen base, 2% [wt/vol] glucose, 2% [wt/vol] agar, and appropriate amino acids except leucine, tryptophan, histidine, and adenine) supplemented with 10 mM 3-amino-1,2,4-triazole to suppress background growth. Positive colonies were isolated, and the cDNA library plasmids were rescued. To confirm the interaction, the cDNA library plasmids were retransformed back into *Saccharomyces cerevisiae* cells with the bait or the empty vector (pGBKT7). Approximately 1×10^6 independent colonies were screened, resulting in one positive clone that was selected for further analysis.

Cloning of full-length LRF gene by 5′ rapid amplification of cDNA ends (RACE). First strand cDNA was synthesized from approximately 2 μg of total RNA from HeLa cells, using the SuperScript II One-Step reverse transcription-PCR (RT-PCR) system (Invitrogen) according to the manufacturer's instructions. The full-length cDNA was subsequently amplified using the primers 5′-AGTGAATTCATGCCTCAGCCTAGTGTAAGC and5′-AATTCTCGAGTTACACCTTTGATGTTGG (underlined sequences are restriction sites appended to the primers) and cloned into the vectors pEGFP-C2, pFLAG-C, and pM3 (containing the GAL4 DNA-binding domain; Ivan Sadowski, University of British Columbia) between the EcoRI/SalI sites. The resulting clones were confirmed by DNA sequencing.

Plasmids. The cDNA encoding N-terminal deletion mutants LRF consisting of amino acid residues 214 to 639 [LRF(214–639)], LRF(349–639), and LRF(451–639) and C-terminal mutants LRF(1–525) and LRF(1–347) were generated by PCR and cloned into the EcoRI/SalI site of the mammalian expression vector pHA-C that is modified from pcDNA3.1/myc-His (Invitrogen) to add the hemagglutinin (HA) epitope tag at the N terminus. Mutant LRF with a deletion of residues 415 to 519 (LRFΔ415-519) and LRFΔ488-504 were generated from the full-length pHA-LRF clone through site-directed mutagenesis using the QuikChange II system (Stratagene). The full-length LRF(1-639) cDNA was cloned into the bacterial expression vector pGEX-KG (coding for a glutathione-Sepharose transferase fusion protein; Gerry Weinmaster, University of California, Los Angeles). The plasmid pIND-LRF was created by subcloning FLAG-LRF(1-639) into the HindIII/SalI site of the vector pIND (Invitrogen), which contains a ponasterone A-inducible promoter. Construction of pFLAG-Luman, pGEX-Luman, pM-Luman, pFLAG-Luman(1-215), and pGEX-Zhangfei (ZF) was described previously (45). The plasmid p3×ERSEII-Luc was created by cloning the linker 5′-AGCTTGCCGATTGGGCCACGTTGGGAGAGCCGATTGGGCCACGTTGGGAGAGCCGATTGGGCCACGTTGGGAGAA that contains three copies of the ERSE-II element into the HindII/BglII sites of the plasmid pGL3-promoter (Promega). The reporter plasmid p5×UPRE-Luc (gift from Ron Prywes, Columbia University) and p5×GAL4-Luc (Ivan Sadowski, University of British Columbia) contains five repeats of the UPRE sequence TGACGTG(G/A) or GAL4 upstream activation sequences, respectively, linked to the coding sequence for firefly (*Photinus pyralis*) luciferase. The pRL-SV40 (where SV40 is simian virus 40) plasmid (Promega) contains the *Renilla* (*Renilla reniformis*) luciferase gene under the control of the SV40 immediate-early promoter. The plasmids expressing the nuclear proteins pEGFP-SF2/ASF, pEGFP-RIP140, and pSG5-HA-GRIP1 (where EGFP is enhanced green fluorescent protein [GFP], RIP140 is nuclear receptor interacting protein 140, and GRIP1 is glucocorticoid receptor interacting protein 1) were generously provided by David Spector, Cold Spring Harbor Laboratories (27); Johanna Zilliacus, Karolinska Institutet (95); and Michael Stallcup, University of Southern California (30), respectively.

Cell culture and transfection. HeLa, human embryonic kidney 293, Rat glial C6, stable-inducible EcR-293/LRF, $LRF^{+/+}$, and $LRF^{-/-}$ mouse embryonic fibroblast (MEF) cells were grown in monolayer culture in Dulbecco's modified Eagle's medium (high glucose) supplemented with 10% (vol/vol) fetal bovine serum (Invitrogen), 100 IU/ml penicillin, and 100 μg/ml streptomycin. All cultures were maintained in a 5% CO_2 humidified atmosphere at 37°C and passaged every 2 to 3 days. Cells were plated 24 h prior to transfection and allowed to grow to 50 to 60% confluence. Cells were transfected by Lipofectamine (Invitrogen) as previously described (44). The proteasome inhibitor, MG132, was used to treat cells for 8 h at a concentration of 5 μM.

Stable-inducible EcR-293/LRF cells were created by transfecting pIND-LRF into EcR-293 cells (Invitrogen). Stable recombinant cells were selected by G418 and zeocin treatment for 30 days. Clonal lines were isolated, and inducible LRF expression was confirmed by Western blotting.

$LRF^{+/+}$ and $LRF^{-/-}$ gene trap knockout MEF cells were extracted from embryos at 12.5 days postcoitus from a $LRF^{+/-} \times LRF^{+/-}$ mating. The LRF gene trap mouse line was made from an embryonic stem cell clone from Bay Genomics (San Francisco), in which a gene-trapping plasmid was inserted into the first intron of the mouse LRF locus and verified by sequencing of the genomic locus.

Western blotting. Detection of LRF was performed using an affinity-purified rabbit polyclonal LRF antibody (RB37), raised against the peptide YENDSVEDLKEVTSISSRKR (custom made by Invitrogen). Other primary antibodies used include affinity-purified polyclonal Luman Rb5660 antibody described previously (40), FLAG monoclonal antibody (M2; Sigma), and a β-actin monoclonal antibody (clone AC-15; Sigma). Blots were visualized using ECL Plus (GE Healthcare) on a Typhoon 9400 Phosphorimager (GE Healthcare).

RNA analysis. Total RNA was isolated with Trizol (Invitrogen) from cell cultures or adult mouse tissues. Synthesis of cDNA was performed using SuperScriptII reverse transcriptase (Invitrogen) and oligo(dT) (Roche). PCR amplification of endogenous mouse LZIP/Luman, LRF, and β-actin or exogenous LRF was performed using the following primers: for mouse LZIP/Luman, 5′-TCAAGCCATGGTGATTGAGA and 5′-CTGAGGACACCCCACATCCT; for endogenous LRF, 5′-AGAAAGCCCAGTATGAAGCTAA and 5′-GGATCATGCTTCACTTATGCTA; for mouse β-actin 5′-GAGAAAATCTGGCACCACACC and 5′-TGCTGATCCACATCTGCTGG; for human β-actin 5′ ATCATTGCTCCTCCTGAGCG and 5′-TGCTGATCCACATCTGCTGG; for exogenous LRF 5′-TGAGTCCTCACTATTAAGTTGAGC and 5′-CCTGCTGGAGTTCGTGACCG (for GFP tag) or 5′-AAGGACGACGATGACAAGGT (for FLAG tag).

qRT-PCR. Quantitative RT-PCR (qRT-PCR) analysis used Sybr Green PCR Master Mix (Applied Biosystems) with primers for human Luman (5′-CCAGGCCATGGTGATTGAG and 5′-GCAGGTACAAGGAGGAGGCAG), human β-actin (5′-ATCATTGCTCCTCCTGAGCG and 5′-TGCTGATCCACATCTGCTGG), mouse Luman/LZIP (5′-GCCTTCTGAGTGGAATCGAGA and 5′-CCGTGATTTCTTCACTGCGTATT), mouse LRF (5′-CAGAATCGGGAGCTGCAGA and 5′-AATCACCATGGCTTGAAGCTTC), mouse ATF4 (5′-TCGGAATGGCCGGCTAT and 5′-TCTCCAACATCCAATCTGTCCC), mouse CHOP (5′-GCAGCGACAGAGCCAGAATAA and 5′-TTCTGCTTTCAGGTGTGGTGG), mouse EDEM (5′-CAGACGAGCTGTGAAAGCCC and 5′-AACCCAATGGCCTGTCTGG), mGRP78/BiP (5′-CAGGCTGGTGTCCTCTCTGG and 5′-CTCCCACAGTTTCAATACCAAGTG), mouse Herp (5′-GCGACATGTTTTGCACCTTGT and 5′-CGGCTGCTCTGTGGATTCA), mouse XBP1 (5′-CGAGCTGGAGCAGCAAGTG and 5′-AAGGCCGTGAGTTTTCTCCC), and mouse Actin (5′-CCTGAACCCTAAGGCCAACC and 5′-CACAGCCTGGATGGCTACG). Samples were run on an ABI 7300 system and sub-

jected to standard curve analysis. Values were analyzed using the ABI 7300 System Sequence Detection Software, version 1.2.2, and are given relative to the wild-type untreated cells. To ensure that appropriate primer-specific products were produced, melting curve analyses were performed on the Sybr green channel using a ramping rate of 1°C/30 s for 60 to 95°C. Data are presented as the averages of three independent repeats.

Pulse-chase assay. At 20 h posttransfection cells were split equally into 6-mm plates and allowed to recover for 16 h. Cells were pulse-labeled in ^{35}S-labeled methionine-cysteine for 1 h and harvested at the indicated time points (see Fig. 5B and 6A). Lysates were immunoprecipitated with monoclonal FLAG antibody M2 (Sigma) and separated on a 12% sodium dodecyl sulfate-polyacrylamide gel electrophoresis (SDS-PAGE) gel. Gels were dried, exposed to a storage phosphorous screen, and visualized on a Typhoon 9400 PhosphorImager.

Coimmunoprecipitation assay. LRF expression in EcR-293/LRF cells was induced with ponasterone A for 24 h with an 8-h treatment of MG132 and brefeldin A. Immunoprecipitations were performed using an M2 FLAG antibody and protein A beads. Western blotting analyses were performed using affinity-purified Luman RB5660 or LRF Rb37 antibody, as described above.

Dual luciferase assays. Cells were transfected as described above. At 16 h posttransfection, the medium was changed, and the cells were allowed to recover for 24 h. Cells were harvested and lysed, and dual luciferase assays were performed according to the manufacturer's protocols (Promega). Luciferase activity was measured using a Turner TD-20e Luminometer and calculated as relative luciferase activity (firefly luciferase/*Renilla* luciferase) to correct for transfection efficiency. Assays were independently repeated at least three times. Data are shown with standard errors.

GST pull-down assays. Glutathione *S*-transferase (GST) fusion proteins were produced in *Escherichia coli* strain BL21(DE3) (Novagen) and were purified using glutathione-Sepharose beads (GE Healthcare) (44, 45). A rabbit reticulocyte in vitro transcription-translation system (TnT; Promega) was used according to the manufacturer's protocol to produce ^{35}S-labeled Luman, HCF-1, LRF and its mutants, and the GAL4 activation domain fused to GFP (as a negative control). Equal amounts of bead-bound proteins were used in all samples as determined by SDS-PAGE against bovine serum albumin standards. GST fusion proteins bound to glutathione-Sepharose 4B beads were incubated for 1 h with 15 μl of in vitro ^{35}S-labeled protein in a total of 150 μl of incubation buffer (140 mM NaCl, 50 mM Tris, pH 8.0, 2 mM Na_3VO_4, 5 mg/ml bovine serum albumin, and 0.5% [vol/vol] Igepal CA-630). Beads were collected by centrifugation, washed, and resuspended in 40 μl of 2× SDS sample buffer. The eluted protein was separated by SDS-PAGE and visualized on a Typhoon 9400 PhosphorImager.

Immunofluorescence confocal microscopy. Cells were fixed for 20 min in 4% paraformaldehyde, permeabilized for 5 min in 1% Triton X-100, and blocked for 60 min in 10% horse serum at room temperature. Primary antibodies were used at the following dilutions: Luman at 1:300, LRF at 1:150, HCF-1.2131 at 1:200, PML-PG-M3 at 1:200 (Santa Cruz), FLAG-M2 at 1:200 (Sigma), and HA-12CA5 at 1:200 (Roche). Secondary Alexa488-, Alexa546-, or Alexa633-conjugated antibodies were used at 1:400 (Invitrogen). Glass coverslips were incubated in antibodies for 60 min at 37°C with 5% CO_2 and were mounted in 50% glycerol with 500 pM DAPI (4′,6′-diamidino-2-phenylindole). Images were captured on a Leica DMRE confocal microscope. Figures were prepared using Adobe Creative Suite CS2.

Nucleotide sequence accession number. The nucleotide sequence of LRF cDNA has been deposited in the GenBank under accession number AY635785.

RESULTS

Identification of the LRF. Luman belongs to the CREB/ATF family of transcription factors and contains a leucine zipper region which is a known protein dimerization motif (1). To identify cellular proteins that interact with Luman, the region (aa 162 to 228) containing the leucine zipper was used as bait in a yeast two-hybrid screen of a human brain cDNA library. Among approximately 1×10^6 independent colonies that were screened, a single cDNA clone was obtained.

The isolated cDNA clone contained an insert of ~1.8 kb. BLAST (http: //www.ncbi.nlm.nih.gov/BLAST/) searches of the GenBank human cDNA database identified overlapping clones comprising a cDNA contig in which the largest open reading frame was 1,920 bp encoding a protein of 639 aa with a predicted molecular mass of 72 kDa. The presumed protein was designated LRF. The full-length open reading frame of LRF was subsequently cloned by 5′ rapid amplification of cDNA ends using template RNAs extracted from HeLa cells. A more recent search of the GenBank human genome database correlated the open reading frame to a GenBank entry (GeneID 153222) that is predicted by a transcriptome analysis (74) to encode an adult retina protein with an unknown function.

LRF has been well conserved through evolution as it shares over 95% sequence identity at the amino acid level with mouse (GenBank GeneID 77128) and rat homologs (GenBank GeneID 303016) (Fig. 1). The apparent structural features of the LRF proteins include a highly acidic region (aa 355 to 399), a typical bZIP region (aa 521 to 576) with a conserved 5-aa spacer between the basic region and the leucine zipper, and a second leucine zipper-like motif (aa 488 to 509) preceding the bZIP motif. In the acidic region, 33 out of the 45 amino acid residues are negatively charged glutamate or aspartate residues.

LRF interacts with Luman in vitro and in vivo. To verify the direct interaction between LRF and Luman, GST pull-down assays were performed. All proteins including two control proteins, HCF-1 and GAL4-GFP (GAL4 activation domain fused to GFP), LRF, and Luman were produced and ^{35}S labeled in rabbit reticulocytes. As shown in Fig. 2A, GST-Luman was able to pull down ^{35}S-labeled HCF-1 (the positive control, lane 4) as well as ^{35}S-LRF (lane 8) but not the negative control, ^{35}S-labeled GAL4-GFP (lane 12). It is known that bZIP proteins can heterodimerize with different bZIP proteins through the leucine-zipper motif. Since LRF was isolated through its interaction with the leucine zipper region of Luman, we asked whether LRF interacts with the leucine zipper of Luman in a specific manner. Therefore, in the same assay, we included ZF, a Luman-related HCF-1 binding protein, which also has a leucine zipper motif (43). While ZF could complex with HCF-1 as expected, it did not bind LRF (Fig. 2A, compare lanes 3 and 7). In a reciprocal GST pull-down assay (Fig. 2B), LRF could pull down Luman efficiently and itself to a lesser degree but not the GAL4-GFP control. These results suggest that LRF interacts with Luman specifically.

To confirm this interaction in the mammalian cellular environment, we carried out a coimmunoprecipitation in EcR-293/LRF cells in which FLAG-tagged LRF can be induced upon addition of ponasterone A to the medium. After a 24-hour induction, cultures were treated with brefeldin A to activate cellular Luman and induce its proteolytic cleavage (40, 62), along with the proteasome inhibitor MG132 for 8 h. Cells were then harvested under nondenaturing conditions, and LRF complexes were precipitated with an anti-FLAG antibody. Only upon LRF induction was the endogenous nuclear form of Luman found in the LRF complex (Fig. 2C).

LRF binds Luman through its C-terminal region. LRF was identified by virtue of its interaction with the leucine zipper region of Luman, which is a known dimerization domain for bZIP proteins. As LRF is also a bZIP protein, it is reasonable to speculate that LRF interacts with Luman through its bZIP domain. To map the region of LRF that is responsible for binding to Luman, a series of deletion mutants of LRF were made (Fig. 2D). In GST pull-down assays using these LRF

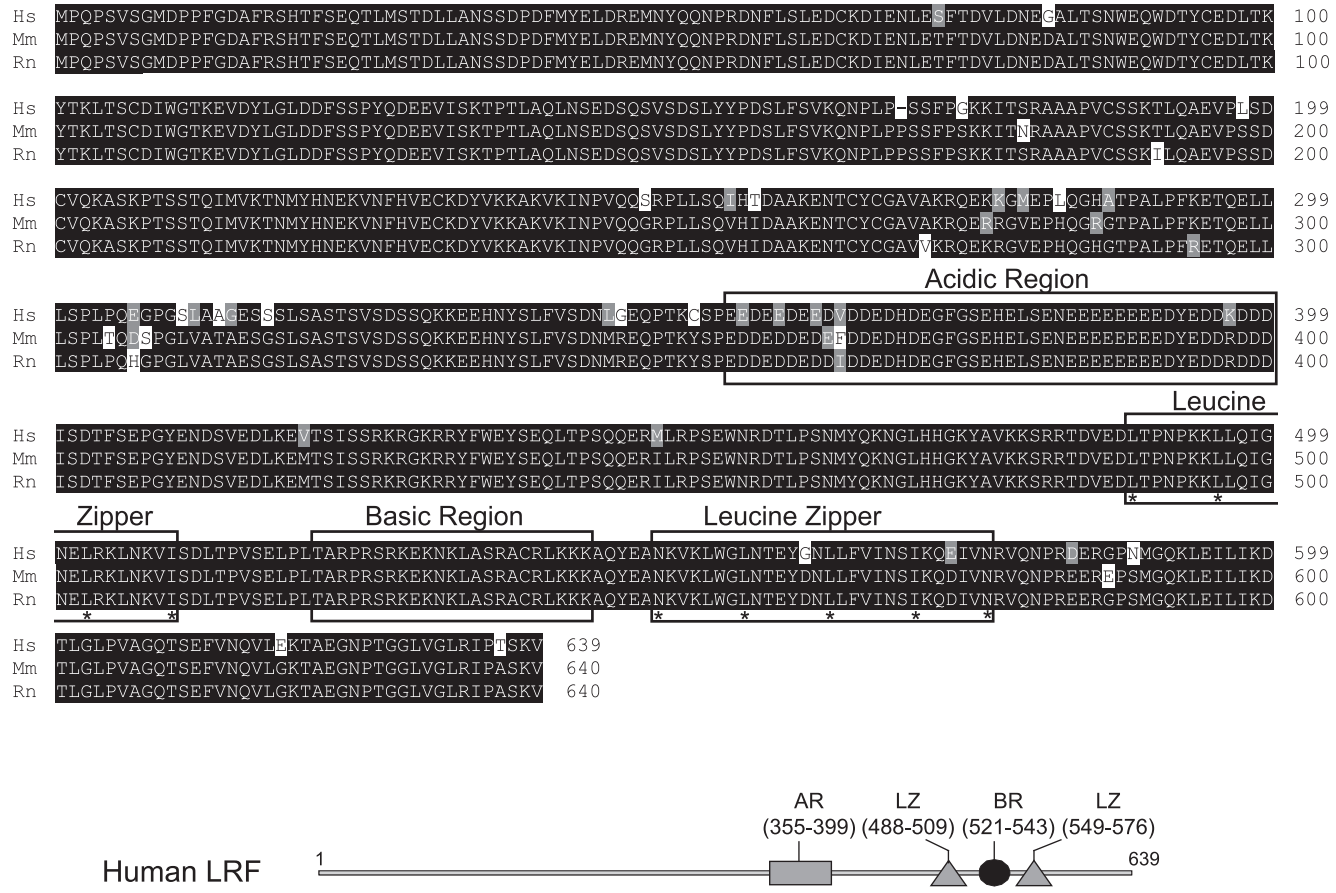

FIG. 1. Amino acid sequence alignment of human LRF and its homologs in mice and rats. Dark-shaded boxes indicate identical amino acids, and gray shading signifies similar amino acid residues. Residues aligned with asterisks are consensus amino acids in the leucine zipper region. The domain structure of LRF is illustrated underneath. Putative domains are denoted as the following: AR, acidic region; BR, basic region; and LZ, leucine zipper.

mutants, the C-terminal region (from aa 451 to 639) that has two leucine zipper-like sequences was sufficient for LRF to bind Luman (Fig. 2D, 4th row). Removal of the C-terminal region (aa 348 to 639) containing both leucine zippers disrupted the interaction between LRF and Luman entirely. Deletion of the second leucine zipper in LRF(1–525) reduced LRF binding to Luman, while removal of the first leucine zipper (aa 488 to 504) abolished the interaction. From these results, we conclude that the first leucine zipper in LRF is indispensable, but both leucine zippers are required for optimal interaction between the two proteins.

LRF recruits Luman into nuclear foci in the cell. To investigate the cellular localization of the LRF protein, fluorescence confocal microscopy studies were carried out. A pEGFP-LRF plasmid expressing the GFP-LRF fusion protein was used to transfect 293 cells, along with plasmids expressing the full-length Luman protein or the N-terminal portion (aa 1 to 215) of Luman. Interestingly, LRF was found exclusively in the nucleus in the form of discrete foci (Fig. 3A).

To examine whether Luman colocalizes with LRF in these cells, 293 cells were cotransfected with pEGFP-LRF and pFLAG-Luman or pFLAG-Luman(1–215). The full-length Luman is a transmembrane protein associated with the ER, and the N-terminal region (aa 1 to 215) of Luman is believed to be the cleavage product and active form of Luman which is localized to the nucleus (40, 62). In the cotransfected cells, the full-length Luman protein remained in the cytoplasm (Fig. 3, compare rows B and D), while N-terminal Luman(1–215) was found to be recruited to the LRF nuclear bodies (Fig. 3, compare rows C and E). Therefore, LRF was able not only to interact with Luman in vivo but also to recruit the nuclear Luman protein into the distinct subnuclear domains.

To investigate the identity of the LRF bodies, we first wanted to rule out that these LRF bodies are artifacts due to overexpression. We have tested different cell lines (e.g., 293, HeLa, and COS7) in our cell transfections, as well as various amounts of plasmid DNA and different expression constructs with weak promoters such as thymidine kinase from herpes simplex virus. LRF was found to form nuclear bodies under all the experimental conditions (date not shown). Next, we sought to compare LRF nuclear bodies to other known nuclear nodules/spots in the literature by confocal microscopy. In terms of morphology, these LRF nuclear bodies appeared to have well-defined and smooth edges. They are also much more spot-like compared to nuclear speckles, which are RNA processing centers (38). The number of LRF bodies ranges from ~20 to ~200 per cell, depending on the cell type (data not shown), and they resemble the well-documented promyelocytic leukemia (PML)

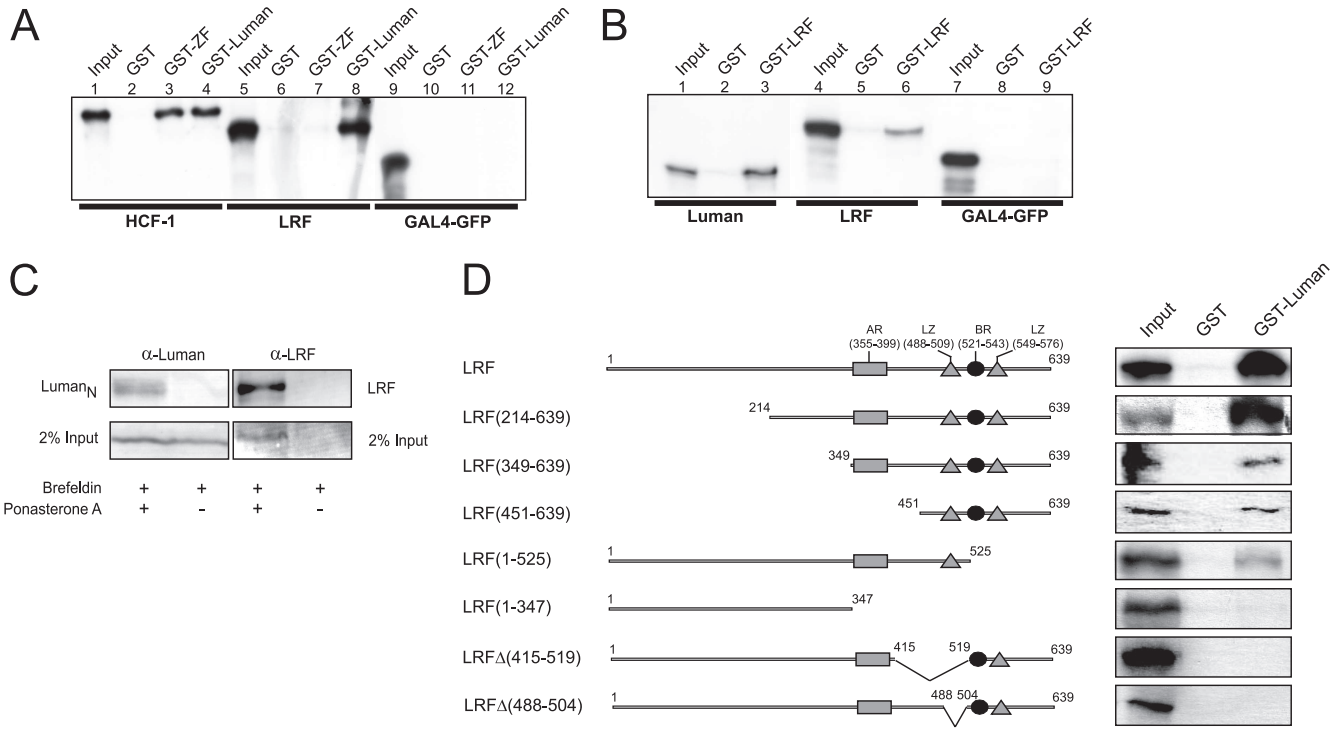

FIG. 2. LRF interacts with Luman specifically through its C-terminal region. (A and B) GST pull-down assays. In vitro translated HCF-1, LRF, and GAL4-GFP were incubated with GST, GST-Luman, or GST-ZF(A) or GST-LRF (B) that were linked with glutathione beads. ^{35}S-labeled HCF-1 was used as a positive control, and ^{35}S-GAL4-GFP was used as a negative control. The binding reactions were subjected to SDS-PAGE and autoradiography. The input lanes have 10% of total ^{35}S-labeled proteins. (C) Immunoprecipitation assays. EcR-293/LRF cells were mock (−) or ponasterone A induced (+), in addition to brefeldin A treatment. Precipitations were performed using the FLAG monoclonal antibody M2 and protein A beads. Western blotting analyses were carried out using antibodies, as indicated at the top of the figure. (D) Mapping of the Luman-binding region in LRF by GST pull-down assays. LRF and its mutants used in the assays are as illustrated in the diagram on the left. In the binding reactions, ^{35}S-labeled LRF was incubated with GST or GST-Luman glutathione beads. Ten percent of the input was included as a reference.

or ND10 bodies (4, 12, 54), RIP140 bodies (95), and GRIP1/TIF2 (transcriptional intermediary factor 2) bodies (30). We found that LRF bodies did not colocalize with nuclear speckles but were juxtaposed with PML or RIP140 bodies. Strikingly, LRF and GRIP1 foci appeared to overlap perfectly (data not shown). These observations led us to conclude that the LRF nuclear bodies are a bona fide subnuclear domain, which is shared with GRIP1.

Coexpression of LRF and Luman in animal tissues. Since LRF is a novel protein, we sought to characterize its tissue distribution; given that multiple human tissue samples are not readily available, we examined LRF expression by qRT-PCR in 10 mouse tissues analyses (adipose, brain, colon, heart, kidney, liver, lung, skeletal muscle, intestine, and testes) (Fig. 4A). While LZIP (the Luman mouse homolog) and LRF coexist in many tissue types at the mRNA level, it appears that they have opposite expression levels when one of the two proteins is in extreme abundance. For instance, LRF is present at very high levels in heart and kidney tissues where Luman/LZIP is low, and the converse is true in the brain. These data seem to imply an antagonistic role of the two proteins.

As with Luman, attempts to survey LRF expression at the protein level in different cell types and tissues proved to be difficult. In our quest for endogenous LRF protein, numerous cell lines were examined. Only one cell line, rat C6 glial cells, has very recently been found to have an appreciable level of LRF by Western blotting using the proteasome inhibitor MG132 and concentrated cell lysates (Fig. 4B). Interestingly, C6 is also the only known cell line that has a considerable amount of endogenous Luman/LZIP protein. We were thus interested in examining the subcellular localization of these two proteins. We found that Luman/LZIP was more readily detectable in all the cells by immunofluorescence microscopy, while LRF appeared to be concentrated in mitotic C6 cells. Surprisingly, we found that both proteins had punctate staining patterns in the mitotic cells. Although less distinct, these foci were very much reminiscent of the nuclear bodies of transfected LRF, especially those of LRF in mitotic C6 cells (Fig. 4B).

Since Luman is known to be involved in the UPR and induced by ER stressors, we examined LRF induction by qRT-PCR in C6 cells under different ER stressor treatments. We found that LRF was induced by the same ER stressors as Luman/LZIP (Fig. 4C).

LRF protein is tightly regulated by the proteasome. To investigate the stability of the LRF protein, we studied the effect of MG132 on the protein levels of transfected GFP- and FLAG-tagged LRF in 293 cells (Fig. 5A). We found that although the levels of LRF mRNA expressed from the plasmids were similar (Fig. 5A, lower panel), the LRF protein levels

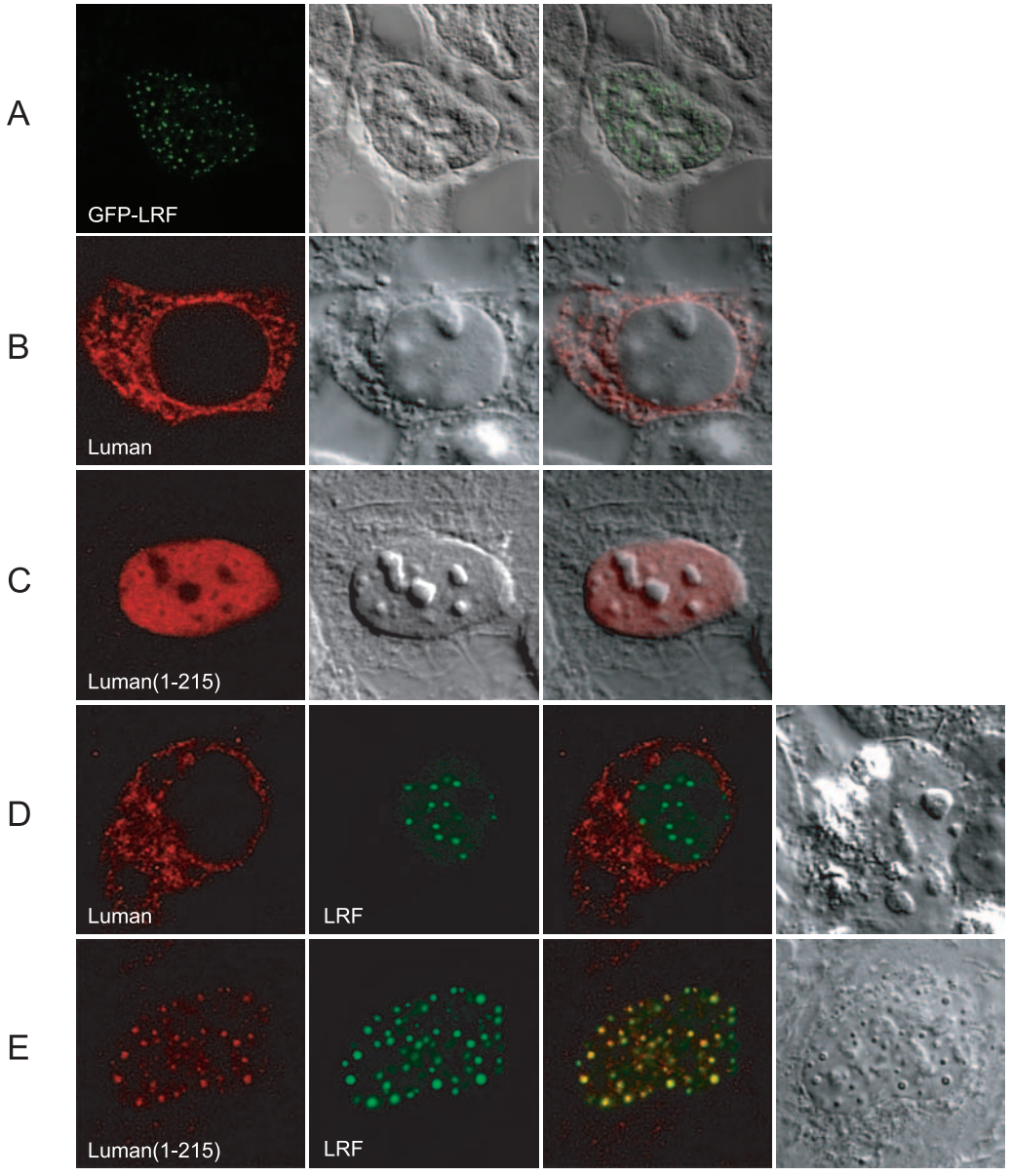

FIG. 3. Confocal microscopic analysis of LRF subcellular localization and its interaction with Luman. 293 cells were either transfected separately with plasmids pEGFP-LRF (A), FLAG-Luman (B), and FLAG-Luman(1–215) (C) or cotransfected with pEGFP-LRF and FLAG-Luman (D) or pEGFP-LRF and FLAG-Luman(1–215) (E). FLAG-Luman proteins were visualized by immunofluorescence labeling using the anti-FLAG monoclonal antibody M2 (Sigma). LRF is shown in green, and the Luman proteins are in red. Images from the green, red, and differential interference contrast channels of the same optical field were captured with a Hamamatsu ORCA-ER digital camera under a Leica DMRE confocal microscope. Composite images of the two channels are shown in the third column.

were drastically different. Cells without MG132 treatment had substantially lower levels of LRF. Among them, FLAG-LRF cells without MG132 treatment completely failed to produce a band (Fig. 5A). It appears that the addition of the larger GFP tag at the amino terminus stabilized LRF within the cell, compared to FLAG-LRF (Fig. 5A, compare lanes 3 and 4 with lanes 5 and 6). It was noted that, with a calculated molecular mass of 72 kDa, the apparent molecular masses of both FLAG-LRF and GFP-LRF were significantly larger, which we believe is likely due to posttranslational modifications of the protein.

To further quantify the stability of LRF protein, a pulse-chase assay was performed on the FLAG-LRF protein. Following a 1-h pulse-labeling of transiently transfected cells, cultures were harvested at multiple time points up to 60 min. Cells were lysed in a nondenaturing buffer and immunoprecipitated with an anti-FLAG antibody. After precipitation, SDS-PAGE, and autoradiography, a single band was found for LRF in each sample (Fig. 5B). The intensity levels of the bands were quantified on a phosphorimager and standardized to the intensity of the time zero sample. Analysis revealed that the half-life of LRF was less than 20 min. In the controls of MG132-treated cells, the half-life of the protein was greater than 60 min, or

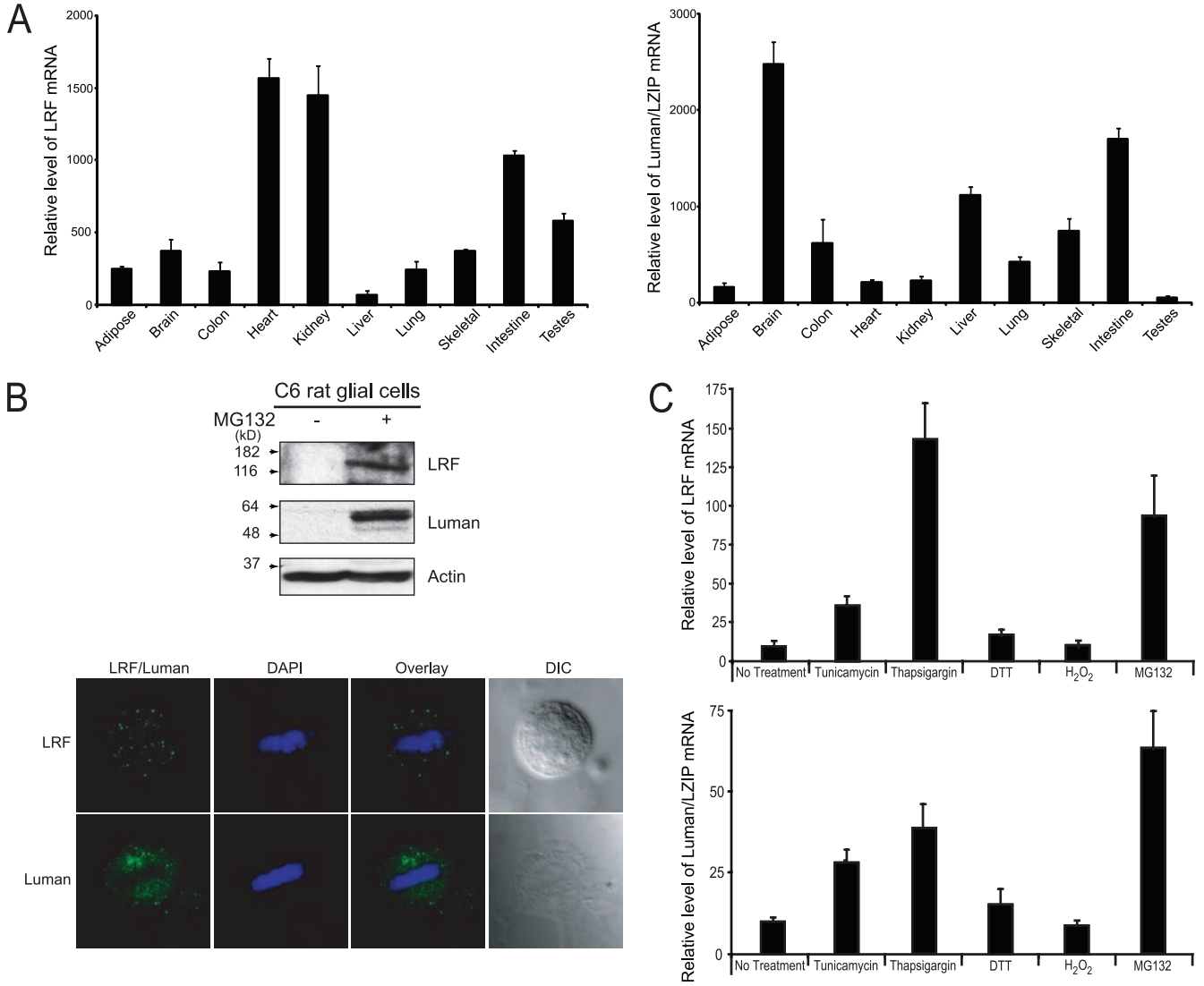

FIG. 4. (A) LRF and Luman/LZIP mRNA distribution patterns in adult mouse tissues by qRT-PCR. mRNA was extracted from adult mouse tissues using the Trizol reagent (Invitrogen) by following manufacturer's protocols, and qRT-PCR was performed using Sybr green PCR Master Mix (Applied Biosystems). Values are normalized to β-actin. (B) Coexpression of LRF and Luman/LZIP in C6 rat glial cells. C6 cells were either mock (−) or MG132 (5 μM; +) treated for 8 h before protein extraction and 10% SDS-PAGE. Lysates were probed for endogenous LRF, Luman/LZIP, and β-actin by Western blotting. Immunofluorescence microscopic analysis of endogenous LRF and Luman/LZIP in C6 cells was carried out using antibodies against LRF and Luman/LZIP. DNA was stained with DAPI. Images were captured under a Leica DMRE confocal microscope. (C). Induction of LRF and Luman/LZIP in C6 cells by ER stress as determined by qRT-PCR. Rat C6 glial cells were treated with 2 μg/ml tunicamycin, 300 nM thapsigargin, 1 mM dithiothreitol (DTT), 300 nM H_2O_2, or 5 μM MG132 for 8 h prior to RNA extraction and qRT-PCR analysis.

three times longer. Together, these results demonstrate that the LRF protein is prone to proteasome degradation and that stability is an important regulatory mechanism of LRF in the cell.

LRF promotes Luman protein degradation. To investigate whether LRF recruitment of the nuclear form of Luman into the LRF foci also impacts the stability of the Luman protein, we cotransfected 293 cells with plasmids expressing the N-terminal Luman(1–215) and LRF or a Luman-binding mutant LRFΔ415–519 and examined the half-life of Luman by pulse-chase assays. We found that the turnover of Luman was more than three times faster when Luman was cotransfected with the full-length LRF than when the blank vector or LRF mutant controls were used (Fig. 6A). The fact that the level of Luman mRNA was not affected by LRF cotransfection (Fig. 6B) suggests that reduction of the Luman protein level was not due to transcriptional repression. In agreement with these results, we noticed that while Luman was readily induced (Fig. 4C) and proteolytically cleaved in cells treated with thapsigargin as detected by Western blotting (40), there was significantly less Luman/LZIP protein in the nucleus of thapsigargin-treated C6 cells visualized by immunofluorescence microscopy (Fig. 6C). Furthermore, when the full-length LRF, but

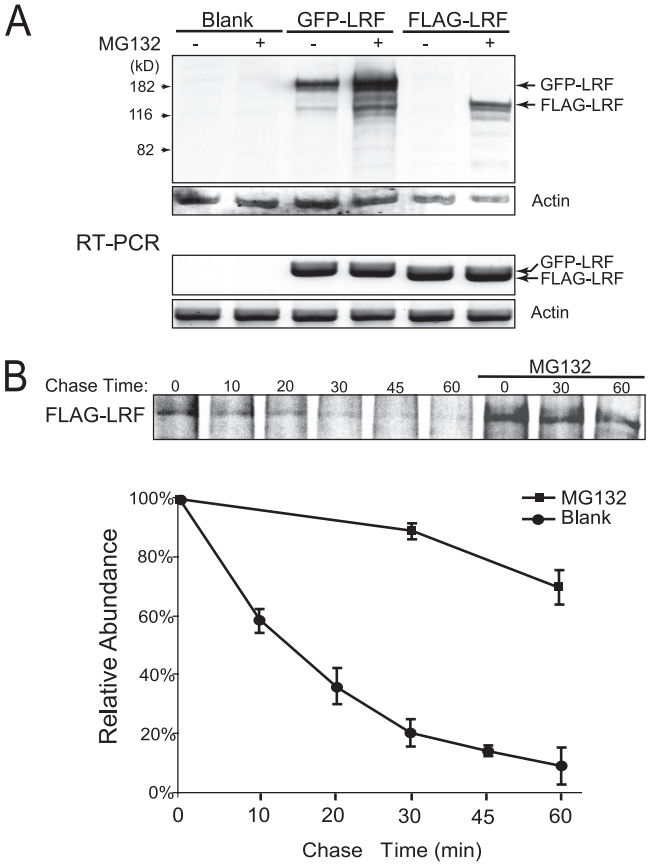

FIG. 5. The LRF protein is rapidly degraded by the proteasome. (A) 293 cells were transiently transfected with 2 μg of pcDNA3.1, pEGFP-LRF, or pFLAG-LRF. Cells were treated with MG132 (5 μM; +) or mock treated (−) for 8 h prior to being harvested for both protein and RNA extraction. Western blot analysis was performed with the LRF antibody RB37 and a β-actin antibody as a loading control. RT-PCR analysis was done using primers specific to the transfected exogenous LRF or endogenous actin. (B) Pulse-chase analysis was performed with pFLAG-LRF transiently transfected 293 cells. Transfected cells were either mock or MG132 (5 μM) treated for 8 h prior to a 1-h pulse-labeling with ^{35}S-labeled methionine-cysteine. Lysates were harvested at 0, 10, 20, 30, 45, and 60 min for untreated samples (blank) and at 0, 30, and 60 min in MG132-treated samples. Lysates were immunoprecipitated with monoclonal FLAG antibody M2 (Sigma) and separated on a 12% SDS-PAGE gel. Images were acquired using a Typhoon 9400 PhosphorImager. Band intensities were analyzed using ImageQuant and expressed as relative abundance compared to time zero values. Data are representative of two independent trials and plotted with standard errors.

not LRFΔ415-519, was overexpressed in C6 cells by transfection, the endogenous Luman/LZIP protein diminished and failed to be detected by immunofluorescence microscopy (Fig. 6C).

LRF represses the activity of Luman during the UPR. To study the functional relevance of the LRF-Luman interaction, we sought to analyze the impact of LRF on the transcription activation function of Luman. Previous studies (11, 40) suggest that Luman may play a role in the ERAD pathway during the UPR and can activate enhancer elements, UPRE and ERSE-II. To analyze the effect of LRF on the Luman response to ER stress, the pcLuman plasmid was used to transfect 293 cells along with a plasmid expressing LRF or the Luman-binding mutant. Using a 5×UPRE luciferase reporter, we found that LRF, but not LRFΔ415–519, could modestly but reproducibly repress the transactivation potential of Luman by 35% (Fig. 7A). A similar level of inhibition was seen when Luman expression was coupled with thapsigargin treatment. Western blot analysis showed that Luman protein levels appeared consistent in the presence and absence of LRF. It should be noted that since Western blotting displays only steady-state protein levels, we cannot rule out the possibility that the observed repression was due to LRF-induced rapid turnover of the Luman protein. Due to the fact that the LRF protein cannot be detected in the absence of MG132, semiquantitative RT-PCR was used to confirm the consistency of LRF levels in all the transfected samples (Fig. 7A, lower panel). When the ERSE-II reporter was examined, however, the LRF repression of the activity of Luman was not significant (Fig. 7B). We postulate that other ERSE-II-activating cellular factors in 293 cells might have masked the repression effect of LRF. To eliminate background activation and check the potential promoter specificity of the LRF repression, the GAL4 upstream activation sequence reporter system was also tested. We found that the transcription potential of Luman was reduced by ~45% by LRF overexpression (Fig. 7C). Thus, the LRF repression of Luman transactivation potential appears to be independent of the promoter context.

To further examine the repressive effect of LRF, thapsigargin-induced activation of UPRE and ERSE-II were examined in LRF wild-type and null MEF cells. Higher levels of reporter activities were seen with both UPRE (150%) and ESRE-II (128%) in LRF$^{-/-}$ cells than in LRF$^{+/+}$ cells (Fig. 7D and E). The two reporters had even greater activity increases in untreated MEF cells, which could be explained by the masking effect of other cellular factors induced by thapsigargin.

LRF is a negative regulator of the mammalian UPR. Next, we sought to study the possible function of LRF in the mammalian UPR using the LRF$^{+/+}$and LRF$^{-/-}$ MEF cells. A time course survey by qRT-PCR indicated that LRF was continuously induced in LRF$^{+/+}$ cells under thapsigargin treatment even though cells started to die after 8 h (Fig. 8A). As expected, no LRF mRNA was detected in LRF$^{-/-}$ samples. We therefore chose the 8-h thapsigargin treatment as the time point and evaluated transcriptional induction of key UPR genes, ATF4, CHOP, EDEM, GRP78, Herp, and XBP1 (Fig. 8B). Out of the six genes examined, CHOP (22%), EDEM (35%), and Herp (32%) showed significant increases in thapsigargin-induced activation in LRF$^{-/-}$ cells, of which EDEM and Herp are known downstream targets of Luman (11, 40) and are believed to play a role in ERAD. Notably, induction of the key ER chaperones GRP78, ATF4, and XBP1 was not affected by LRF deficiency. Thus, the enhancement of EDEM and Herp transcription may be the outcome of the alleviation of LRF repression on endogenous Luman/LZIP in the LRF$^{-/-}$ cells that led to augmentation of its downstream gene expression.

Exclusion of HCF-1 from LRF nuclear bodies. Since Luman is also known to interact with HCF-1, we were interested to investigate whether LRF can also recruit HCF-1 into the discrete nuclear foci along with Luman. We transfected 293 cells with pEGFP-LRF or pFLAG-Luman(1–215) alone or cotrans-

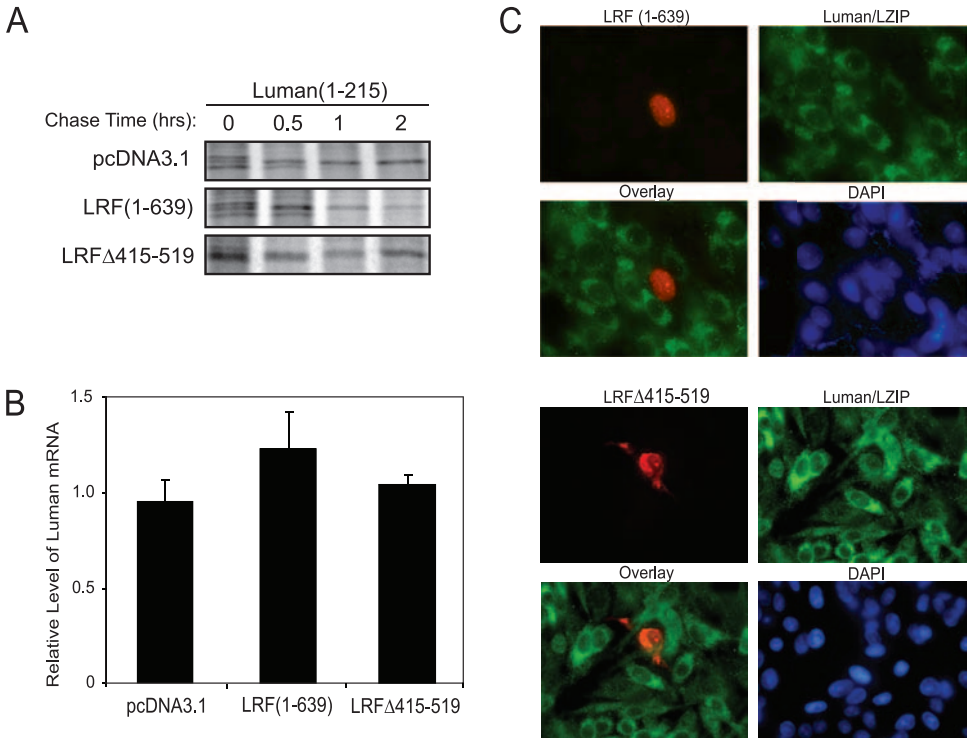

FIG. 6. LRF promotes protein degradation of Luman. (A) Pulse-chase analysis was performed on 293 cells transfected with plasmids expressing FLAG-Luman(1–215) along with LRF(1–639) or LRFΔ414–519. The blank vector pcDNA3.1 was used as a negative control. At 24 h posttransfection cells were split evenly into four plates and allowed to recover for 16 h. Cells were pulse-labeled with ^{35}S-labeled methionine-cysteine for 1 h, and harvested at 0, 0.5, 1, and 2 h postlabeling. Lysates were immunoprecipitated with the FLAG monoclonal antibody M2 (Sigma), and data were analyzed on a Typhoon 9400 PhosphorImager. (B) 293 cells were transfected for 8 h with plasmids as mentioned above. Total cellular RNA was harvested 24 h posttransfection. qRT-PCR of Luman was performed, and the values were standardized to β-actin. (C) C6 glial cells were transfected with plasmids expressing FLAG-LRF(1–639) or the Luman-binding mutant HA-LRFΔ414–519 and treated for 8 h with 5 μM MG132 and 300 nM thapsigargin. FLAG-LRF(1–639) was visualized using the FLAG monoclonal antibody M2 (Sigma) and HA-LRFΔ414–519 with HA-12CA5 (Roche), while endogenous Luman/LZIP was detected with polyclonal antibody 80.3 by immunofluorescence microscopy. Images are captured from multiple channels of the same optical field.

fected the cells with both plasmids and checked the subcellular localization of endogenous HCF-1. Immunofluorescence confocal microscopy showed that LRF did not colocalize with HCF-1 in the absence (Fig. 9, I) or the presence of Luman (Fig. 9, III). Although the N-terminal Luman colocalized with HCF-1 almost perfectly without LRF (Fig. 9, II), upon transfection of LRF, Luman was recruited to the LRF nuclear bodies while HCF-1 was not (Fig. 9, III). A closer examination of the confocal microscopic images revealed that the majority of HCF-1 appeared to be excluded from the LRF bodies (Fig. 9, insets in I and III).

DISCUSSION

In this study we report the discovery of a novel cellular protein, LRF, that interacts with the transcription factor Luman (13, 42, 44–47). Our data suggest that LRF is a negative regulator in the mammalian UPR, especially in the EDEM- and Herp-related ERAD pathway. LRF not only promotes Luman protein degradation through direct binding but also recruits the nuclear Luman protein to discrete nuclear foci and represses its transactivation potential. In addition to accelerating Luman turnover, a key mechanism of LRF repression may be sequestration of Luman in LRF nuclear bodies, thereby excluding cofactors, such as HCF-1, that are required for Luman transactivation. We thus believe that LRF represents another level of control of Luman after its proteolytic cleavage and translocation to the nucleus.

LRF is predicted to be a protein of 639 aa that is extremely well conserved in humans and rodents (Fig. 1). This high level of conservation during the course of evolution suggests a critical cellular role for LRF. Similar to Luman (40), the level of LRF in the cells appears to be tightly regulated by proteasomes, since the proteasome inhibitor MG132 significantly improved the stability of the protein (Fig. 5). The very short half-life of LRF (~20 min) agrees with the observation that the LRF protein is normally present at very low levels, if at all, in most cell types. Not surprisingly, LRF also promotes degradation of Luman (Fig. 6), which may be one of the mechanisms of LRF negative regulation of Luman. It is worth noting that, in this regard, LRF is very much reminiscent of XBP1u in its relation to XBP1s. Like LRF, the unstable protein XBP1u selectively binds XBP1s through the leucine zipper motif and represses the transactivation activity of XBP1s by accelerating its proteasomal degradation (94).

It is now being increasingly appreciated that the cellular nucleus is functionally compartmentalized and that proteins are targeted to discrete subdomains within the nucleus to per-

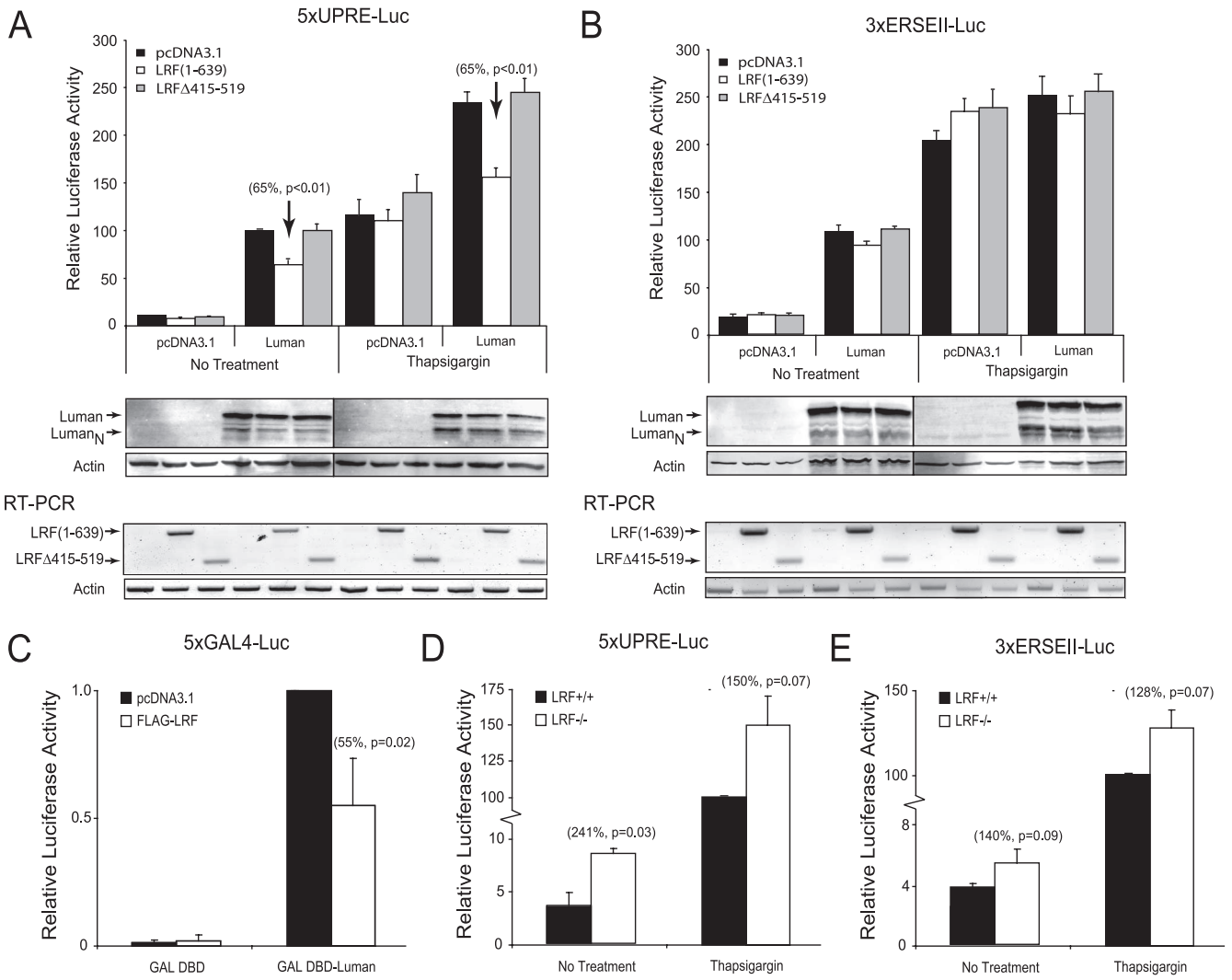

FIG. 7. LRF represses Luman activation of the unfolded protein response. (A and B) 293 cells were transfected with 1 μg of the plasmids pcLuman, pFLAG-LRF, and pHA-LRFΔ415–519, along with the reporter plasmids p5×UPRE-Luc (250 ng) (A) or p3×ERSE-II-Luc (B) as well as pRL-SV40 (50 ng). The parental vector pcDNA3.1 was used as a control. Samples were either mock treated or treated with thapsigargin (300 nM) for 8 h. Dual luciferase assays were performed, and values are presented with standard errors. Western blotting analyses were performed to confirm equal concentrations of the effector protein in the samples, with β-actin used as a loading control. Semiquantitative RT-PCR for transfected exogenous LRF was performed to verify equivalent levels of LRF expression in the samples, with actin as a control. (C) 293 cells were transfected with 1 μg of the empty vector pM1 or the plasmid pM-Luman that encodes a GAL4 DNA-binding domain (GAL DBD) fusion protein of Luman, along with the reporter plasmids p5×GAL-Luc (250 ng) and pRL-SV40 (50 ng). Dual luciferase assays were carried out as described above. (D and E) Dual luciferase assays in $LRF^{+/+}$ and $LRF^{-/-}$ MEF cells either mock treated or treated with thapsigargin (300 nM) for 8 h, as described in panels A and B. Percentage values are of the pcDNA3.1 or $LRF^{+/+}$ controls, shown with the *P* value of a Student's *t* test.

form specialized functions. The LRF nuclear bodies appear to be different from other commonly known subnuclear structures, including nucleoli, nuclear speckles, paraspeckles, cajal bodies, gems, and PML/ND10 bodies. These nuclear bodies, although not bound by membranes, form distinct compartments within the nucleus and contain sets of proteins with specialized functions, such as DNA replication and repair, transcription, RNA processing, gene silencing, and protein degradation (reviewed in references 9, 10, 37, 38, and 96).

In relation to other well-documented nuclear foci, LRF nuclear bodies do not resemble nuclear speckles. The apparent juxtaposition of LRF with PML/ND10 and RIP140 may suggest that they are all tethered to an unknown structure in the nucleus. The discovery of the perfect colocalization of LRF with GRIP1 in the nuclear foci (data not shown) may be of particular importance since GRIP1 is a known nuclear receptor (NR) coactivator (22, 81). One of the hallmarks of NR coactivators is the presence of the NR box, a stretch of amino acids with the sequence LXXLL, where X represents any amino acid. Sequence analysis failed to identify any putative NR boxes within LRF; however, Luman is known to possess two LXXLL motifs in its N terminus. It has been demonstrated that these regions are important to the activation potential of Luman when fused to the GAL4 DNA-binding domain (47). Perhaps recruitment of Luman to these LRF nuclear bodies may not only repress the transactivation function of Luman but

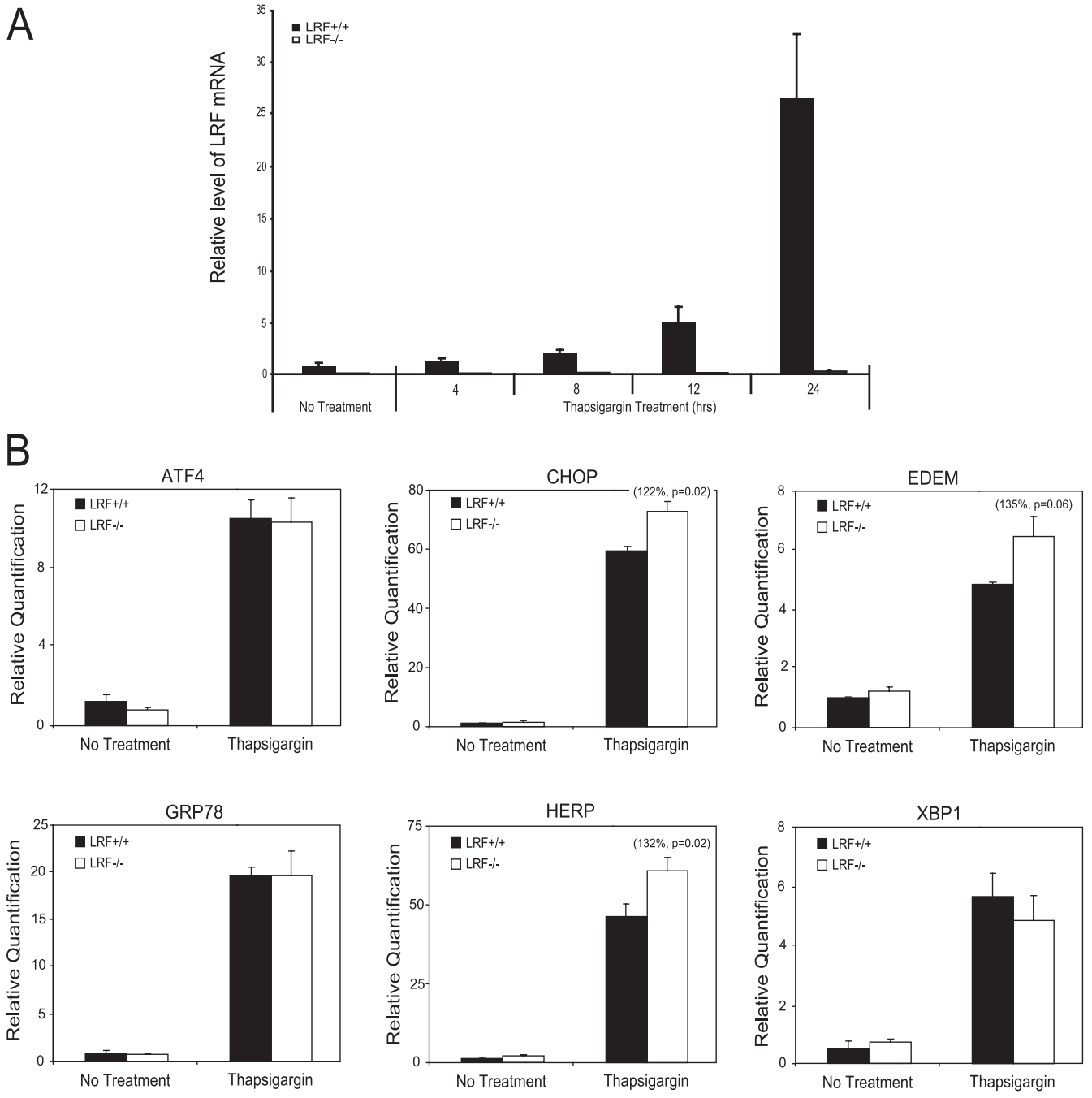

FIG. 8. LRF is a negative regulator of the mammalian UPR. (A) Induction of LRF in MEF cells analyzed by qRT-PCR. The LRF MEF cells were treated with 300 nM thapsigargin for 0, 4, 8, 12, and 24 h. (B) Comparative analysis of key UPR gene induction in $LRF^{+/+}$ and $LRF^{-/-}$ MEF cells. MEF cells were either mock treated or treated with thapsigargin (300 nM) for 8 h. qRT-PCR analyses of ATF4, CHOP, EDEM, GRP78, Herp, and XBP1 were performed using Sybr green mix on an ABI 7300 system, with β-actin as a reference. Percentage values are of the $LRF^{+/+}$ control, shown with the *P* value of a Student's *t* test.

might also render Luman a separate function by allowing it to interact with other NRs and coactivators also present in these foci.

It is worth noting that, through our persistent effort, both endogenous LRF and Luman/LZIP were found in C6 rat glial cells (Fig. 4B). The punctate staining patterns of both proteins in mitotic cells during metaphase were especially encouraging. Unfortunately, we could not reliably determine whether the LRF and Luman/LZIP proteins colocalized in C6 cells, since all our LRF and Luman/LZIP antibodies have the same host origin. At metaphase of the cell cycle, nuclear envelope is already dissolved. It is thus possible for the nonproteolytically processed Luman to interact with LRF. It should also be pointed out, however, that Luman may not be localized in LRF

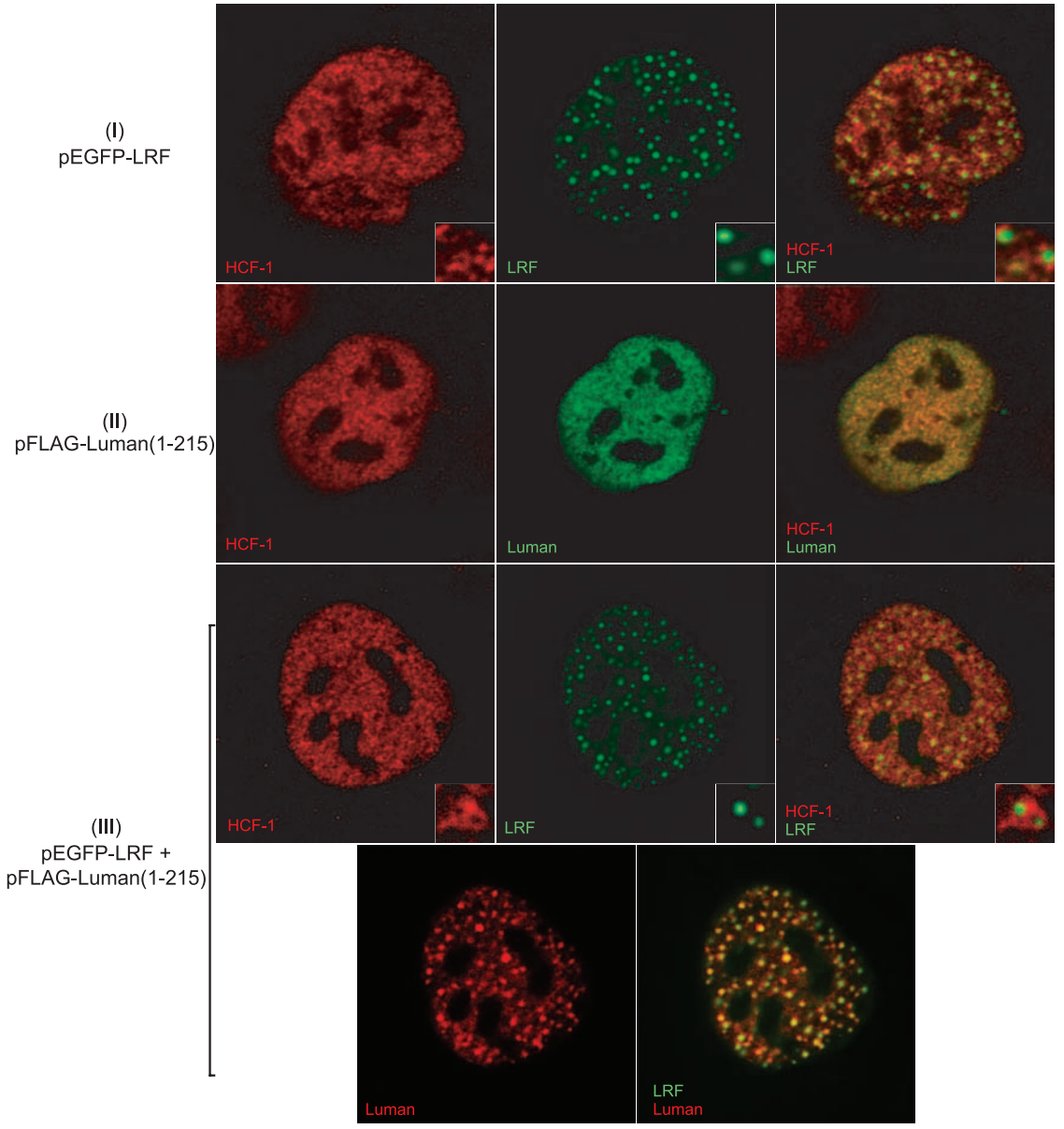

FIG. 9. Exclusion of HCF-1 in the LRF nuclear bodies in the presence or absence of Luman. The 293 cells were either transfected separately with pEGFP-LRF (I) or pFLAG-Luman(1–215) alone (II) or with both plasmids (III). FLAG-Luman(1–215) was visualized using M2 (Sigma) monoclonal antibody against FLAG, while endogenous HCF-1 was detected by polyclonal antibody 2131 (36). The displayed images in each set are captured from multiple channels of the same optical field. Inset images of I and III show regions at higher magnification.

bodies under the "normal" conditions. We noticed that the level of LRF was still very low in the C6 cells (estimated to be 10-fold lower than Luman/LZIP). This might explain why these endogenous LRF nuclear bodies were not as distinct as those in transfected cells. It is possible that LRF forms visible nuclear bodies only under certain cellular conditions when the level of LRF protein reaches a threshold.

Luman as a transcription factor is normally bound to the ER through a C-terminal transmembrane domain, with all the known functional domains facing the cytosol. During the UPR, Luman is believed to be cleaved by regulated intramembrane proteolysis (40, 62), and the N-terminal Luman translocates to the nucleus, turning on downstream targets. Therefore, recruitment of nuclear Luman into specific subnuclear domains by LRF should represent another level of regulation for Luman, subsequent to the proteolysis event in the cytoplasm. Although both LRF and HCF-1 are proteins that interact with Luman in the nucleus, they are potentially two antagonizing forces that regulate the function of Luman, with HCF-1 being the positive cofactor promoting transcription activation by Luman and LRF being a repressor. With current data suggesting that HCF-1 is a ubiquitous cell cycle regulator (28, 31, 77), LRF is more likely to provide tissue specificity that fine-tunes the activity of Luman.

As a working model for the function of Luman recruitment into LRF nuclear bodies, we propose that once proteolytically

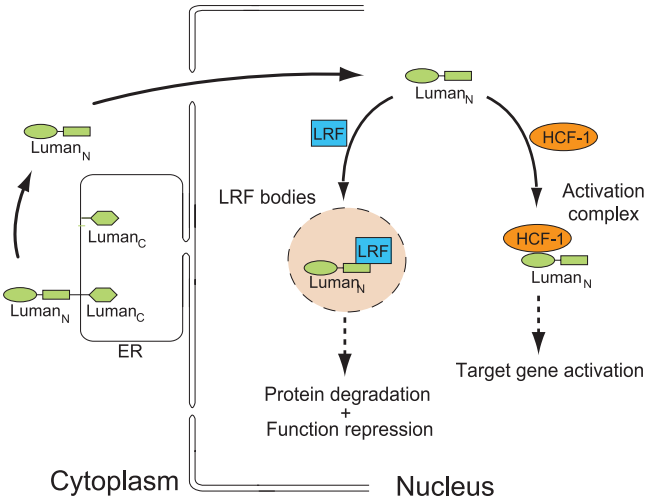

FIG. 10. Working model for the cellular function of Luman recruitment into the LRF nuclear bodies. Luman is a type II transmembrane protein which is normally bound to the ER. During cellular stress responses such as the UPR, Luman undergoes regulated intramembrane proteolysis, and subsequently the N-terminal region of Luman translocates to the nucleus. In the absence of interaction with LRF, nuclear Luman binds to the cofactor HCF-1 and forms a transcription activation complex, leading to the activation of downstream target genes, such as the UPR-related Herp and EDEM. At a point of the UPR where the cellular environment changes and the level of LRF in the nucleus rises to a threshold, Luman may be recruited in the LRF bodies and sequestered from HCF-1, which results in accelerated proteasomal degradation and repression of the transactivation function of Luman.

processed Luman translocates to the nucleus, it may first associate with HCF-1 and form a transcription activation complex, turning on downstream target genes such as ER stress-related Herp and EDEM (11, 40) (Fig. 10). At a certain point of the UPR where the cellular environment changes and the level of LRF in the nucleus rises to a threshold, Luman may be recruited into the LRF nuclear bodies. Translocation of Luman into these LRF nuclear bodies represses its transactivation potential, possibly by sequestering it from essential cofactors (such as HCF-1) and by promoting Luman protein degradation by the proteasome. After the cellular response is near completion, both LRF and Luman may be rapidly degraded. With the availability of a newly established LRF gene knockout mouse line, this hypothesis is being tested.

ACKNOWLEDGMENTS

We thank Amanda Martyn for providing LRF knockout mouse tissues and for her help in producing the MEF cells as well as critical reading of the manuscript. We thank Thomas Kristie for the 2131 antibody against HCF-1, David Spector for pEGFP-SF2/ASF, Ivan Sadowski for p5×GAL4, Johanna Zilliacus for pEGFP-RIP140, and Michael Stallcup for pSG5-HA-GRIP1 plasmids. Y.L. contributed the data in Fig. 6C; G.L. provided technical assistance as well as conceptual help in the early stages of this project. The rest of the work was performed by T.E.A.

This work was supported by funds from the Canadian Institutes for Health Research and the Canadian Foundation for Innovation to R.L.

REFERENCES

1. **Alber, T.** 1992. Structure of the leucine zipper. Curr. Opin. Genet. Dev. **2:**205–210.
2. **Bernales, S., F. R. Papa, and P. Walter.** 2006. Intracellular signaling by the unfolded protein response. Annu. Rev. Cell Dev. Biol. **22:**487–508.
3. **Blot, G., S. Lopez-Verges, C. Treand, N. J. Kubat, D. Delcroix-Genete, S. Emiliani, R. Benarous, and C. Berlioz-Torrent.** 2006. Luman, a new partner of HIV-1 TMgp41, interferes with Tat-mediated transcription of the HIV-1 LTR. J. Mol. Biol. **364:**1034–1047.
4. **Borden, K. L.** 2002. Pondering the promyelocytic leukemia protein (PML) puzzle: possible functions for PML nuclear bodies. Mol. Cell. Biol. **22:**5259–5269.
5. **Brown, M. S., and J. L. Goldstein.** 1997. The SREBP pathway: regulation of cholesterol metabolism by proteolysis of a membrane-bound transcription factor. Cell **89:**331–340.
6. **Calfon, M., H. Zeng, F. Urano, J. H. Till, S. R. Hubbard, H. P. Harding, S. G. Clark, and D. Ron.** 2002. IRE1 couples endoplasmic reticulum load to secretory capacity by processing the XBP-1 mRNA. Nature **415:**92–96.
7. **Cao, G., X. Ni, M. Jiang, Y. Ma, H. Cheng, L. Guo, C. Ji, S. Gu, Y. Xie, and Y. Mao.** 2002. Molecular cloning and characterization of a novel human cAMP response element-binding (CREB) gene (CREB4). J. Hum. Genet. **47:**373–376.
8. **Chin, K. T., H. J. Zhou, C. M. Wong, J. M. Lee, C. P. Chan, B. Q. Qiang, J. G. Yuan, I. O. Ng, and D. Y. Jin.** 2005. The liver-enriched transcription factor CREB-H is a growth suppressor protein underexpressed in hepatocellular carcinoma. Nucleic Acids Res. **33:**1859–1873.
9. **Chubb, J. R., and W. A. Bickmore.** 2003. Considering nuclear compartmentalization in the light of nuclear dynamics. Cell **112:**403–406.
10. **Cioce, M., and A. I. Lamond.** 2005. Cajal bodies: a long history of discovery. Annual review of cell and developmental biology **21:**105–131.
11. **DenBoer, L. M., P. W. Hardy-Smith, M. R. Hogan, G. P. Cockram, T. E. Audas, and R. Lu.** 2005. Luman is capable of binding and activating transcription from the unfolded protein response element. Biochem. Biophys. Res. Commun. **331:**113–119.
12. **Eskiw, C. H., and D. P. Bazett-Jones.** 2002. The promyelocytic leukemia nuclear body: sites of activity? Biochem. Cell Biol. **80:**301–310.
13. **Freiman, R. N., and W. Herr.** 1997. Viral mimicry: common mode of association with HCF by VP16 and the cellular protein LZIP. Genes Dev. **11:**3122–3137.
14. **Harding, H. P., I. Novoa, Y. Zhang, H. Zeng, R. Wek, M. Schapira, and D. Ron.** 2000. Regulated translation initiation controls stress-induced gene expression in mammalian cells. Mol. Cell **6:**1099–1108.
15. **Harding, H. P., H. Zeng, Y. Zhang, R. Jungries, P. Chung, H. Plesken, D. D. Sabatini, and D. Ron.** 2001. Diabetes mellitus and exocrine pancreatic dysfunction in Perk$^{-/-}$ mice reveals a role for translational control in secretory cell survival. Mol. Cell **7:**1153–1163.
16. **Harding, H. P., Y. Zhang, A. Bertolotti, H. Zeng, and D. Ron.** 2000. Perk is essential for translational regulation and cell survival during the unfolded protein response. Mol. Cell **5:**897–904.
17. **Harding, H. P., Y. Zhang, and D. Ron.** 1999. Protein translation and folding are coupled by an endoplasmic-reticulum-resident kinase. Nature **397:**271–274.
18. **Harding, H. P., Y. Zhang, H. Zeng, I. Novoa, P. D. Lu, M. Calfon, N. Sadri, C. Yun, B. Popko, R. Paules, D. F. Stojdl, J. C. Bell, T. Hettmann, J. M. Leiden, and D. Ron.** 2003. An integrated stress response regulates amino acid metabolism and resistance to oxidative stress. Mol. Cell **11:**619–633.
19. **Haze, K., T. Okada, H. Yoshida, H. Yanagi, T. Yura, M. Negishi, and K. Mori.** 2001. Identification of the G13 (cAMP-response-element-binding protein-related protein) gene product related to activating transcription factor 6 as a transcriptional activator of the mammalian unfolded protein response. Biochem. J. **355:**19–28.
20. **Haze, K., H. Yoshida, H. Yanagi, T. Yura, and K. Mori.** 1999. Mammalian transcription factor ATF6 is synthesized as a transmembrane protein and activated by proteolysis in response to endoplasmic reticulum stress. Mol. Biol. Cell **10:**3787–3799.
21. **Hogan, M. R., G. P. Cockram, and R. Lu.** 2006. Cooperative interaction of Zhangfei and ATF4 in transactivation of the cyclic AMP response element. FEBS Lett. **580:**58–62.
22. **Hong, H., K. Kohli, M. J. Garabedian, and M. R. Stallcup.** 1997. GRIP1, a transcriptional coactivator for the AF-2 transactivation domain of steroid, thyroid, retinoid, and vitamin D receptors. Mol. Cell. Biol. **17:**2735–2744.
23. **Hong, M., S. Luo, P. Baumeister, J. M. Huang, R. K. Gogia, M. Li, and A. S. Lee.** 2004. Underglycosylation of ATF6 as a novel sensing mechanism for activation of the unfolded protein response. J. Biol. Chem. **279:**11354–11363.
24. **Honma, Y., K. Kanazawa, T. Mori, Y. Tanno, M. Tojo, H. Kiyosawa, J. Takeda, T. Nikaido, T. Tsukamoto, S. Yokoya, and A. Wanaka.** 1999. Identification of a novel gene, OASIS, which encodes for a putative CREB/ATF family transcription factor in the long-term cultured astrocytes and gliotic tissue. Brain Res. Mol. Brain Res. **69:**93–103.
25. **Jang, S. W., Y. S. Kim, Y. R. Kim, H. J. Sung, and J. Ko.** 2007. Regulation of human LZIP expression by NF-kappaB and its involvement in monocyte cell migration induced by Lkn-1. J. Biol. Chem. **282:**11092–11100.
26. **Jiang, H. Y., S. A. Wek, B. C. McGrath, D. Lu, T. Hai, H. P. Harding, X. Wang, D. Ron, D. R. Cavener, and R. C. Wek.** 2004. Activating transcription

factor 3 is integral to the eukaryotic initiation factor 2 kinase stress response. Mol. Cell. Biol. **24:**1365–1377.
27. **Jimenez-Garcia, L. F., and D. L. Spector.** 1993. In vivo evidence that transcription and splicing are coordinated by a recruiting mechanism. Cell **73:** 47–59.
28. **Julien, E., and W. Herr.** 2004. A switch in mitotic histone H4 lysine 20 methylation status is linked to M phase defects upon loss of HCF-1. Mol. Cell **14:**713–725.
29. **Kaneko, M., M. Ishiguro, Y. Niinuma, M. Uesugi, and Y. Nomura.** 2002. Human HRD1 protects against ER stress-induced apoptosis through ER-associated degradation. FEBS Lett. **532:**147–152.
30. **Kim, J. H., H. Li, and M. R. Stallcup.** 2003. CoCoA, a nuclear receptor coactivator which acts through an N-terminal activation domain of p160 coactivators. Mol. Cell **12:**1537–1549.
31. **Knez, J., D. Piluso, P. Bilan, and J. P. Capone.** 2006. Host cell factor-1 and E2F4 interact via multiple determinants in each protein. Mol. Cell. Biochem. **288:**79–90.
32. **Kokame, K., K. L. Agarwala, H. Kato, and T. Miyata.** 2000. Herp, a new ubiquitin-like membrane protein induced by endoplasmic reticulum stress. J. Biol. Chem. **275:**32846–32853.
33. **Kondo, S., T. Murakami, K. Tatsumi, M. Ogata, S. Kanemoto, K. Otori, K. Iseki, A. Wanaka, and K. Imaizumi.** 2005. OASIS, a CREB/ATF-family member, modulates UPR signalling in astrocytes. Nat. Cell Biol. **7:**186–194.
34. **Kondo, S., A. Saito, S. Hino, T. Murakami, M. Ogata, S. Kanemoto, S. Nara, A. Yamashita, K. Yoshinaga, H. Hara, and K. Imaizumi.** 2007. BBF2H7, a novel transmembrane bZIP transcription factor, is a new type of endoplasmic reticulum stress transducer. Mol. Cell. Biol. **27:**1716–1729.
35. **Kopito, R. R.** 1997. ER quality control: the cytoplasmic connection. Cell **88:**427–430.
36. **Kristie, T. M., and P. A. Sharp.** 1993. Purification of the cellular C1 factor required for the stable recognition of the Oct-1 homeodomain by the herpes simplex virus alpha-trans-induction factor (VP16). J. Biol. Chem. **268:**6525–6534.
37. **Lam, Y. W., L. Trinkle-Mulcahy, and A. I. Lamond.** 2005. The nucleolus. J. Cell Sci. **118:**1335–1337.
38. **Lamond, A. I., and D. L. Spector.** 2003. Nuclear speckles: a model for nuclear organelles. Nat. Rev. Mol. Cell Biol. **4:**605–612.
39. **Lee, K., W. Tirasophon, X. Shen, M. Michalak, R. Prywes, T. Okada, H. Yoshida, K. Mori, and R. J. Kaufman.** 2002. IRE1-mediated unconventional mRNA splicing and S2P-mediated ATF6 cleavage merge to regulate XBP1 in signaling the unfolded protein response. Genes Dev. **16:**452–466.
40. **Liang, G., T. E. Audas, Y. Li, G. P. Cockram, J. D. Dean, A. C. Martyn, K. Kokame, and R. Lu.** 2006. Luman/CREB3 induces transcription of the endoplasmic reticulum (ER) stress response protein Herp through an ER stress response element. Mol. Cell. Biol. **26:**7999–8010.
41. **Lu, P. D., H. P. Harding, and D. Ron.** 2004. Translation reinitiation at alternative open reading frames regulates gene expression in an integrated stress response. J. Cell Biol. **167:**27–33.
42. **Lu, R., and V. Misra.** 2000. Potential role for luman, the cellular homologue of herpes simplex virus VP16 (alpha gene trans-inducing factor), in herpesvirus latency. J. Virol. **74:**934–943.
43. **Lu, R., and V. Misra.** 2000. Zhangfei: a second cellular protein interacts with herpes simplex virus accessory factor HCF in a manner similar to Luman and VP16. Nucleic Acids Res. **28:**2446–2454.
44. **Lu, R., P. Yang, P. O'Hare, and V. Misra.** 1997. Luman, a new member of the CREB/ATF family, binds to herpes simplex virus VP16-associated host cellular factor. Mol. Cell. Biol. **17:**5117–5126.
45. **Lu, R., P. Yang, S. Padmakumar, and V. Misra.** 1998. The herpesvirus transactivator VP16 mimics a human basic domain leucine zipper protein, Luman, in its interaction with HCF. J. Virol. **72:**6291–6297.
46. **Luciano, R. L., and A. C. Wilson.** 2002. An activation domain in the C-terminal subunit of HCF-1 is important for transactivation by VP16 and LZIP. Proc. Natl. Acad. Sci. USA **99:**13403–13408.
47. **Luciano, R. L., and A. C. Wilson.** 2000. N-terminal transcriptional activation domain of LZIP comprises two LxxLL motifs and the host cell factor-1 binding motif. Proc. Natl. Acad. Sci. USA **97:**10757–10762.
48. **Ma, Y., J. W. Brewer, J. A. Diehl, and L. M. Hendershot.** 2002. Two distinct stress signaling pathways converge upon the CHOP promoter during the mammalian unfolded protein response. J. Mol. Biol. **318:**1351–1365.
49. **Marciniak, S. J., and D. Ron.** 2006. Endoplasmic reticulum stress signaling in disease. Physiol. Rev. **86:**1133–1149.
50. **Molinari, M., V. Calanca, C. Galli, P. Lucca, and P. Paganetti.** 2003. Role of EDEM in the release of misfolded glycoproteins from the calnexin cycle. Science **299:**1397–1400.
51. **Mori, K.** 2000. Tripartite management of unfolded proteins in the endoplasmic reticulum. Cell **101:**451–454.
52. **Murakami, T., S. Kondo, M. Ogata, S. Kanemoto, A. Saito, A. Wanaka, and K. Imaizumi.** 2006. Cleavage of the membrane-bound transcription factor OASIS in response to endoplasmic reticulum stress. J. Neurochem. **96:**1090–1100.
53. **Nagamori, I., N. Yabuta, T. Fujii, H. Tanaka, K. Yomogida, Y. Nishimune, and H. Nojima.** 2005. Tisp40, a spermatid specific bZip transcription factor, functions by binding to the unfolded protein response element via the Rip pathway. Genes Cells **10:**575–594.
54. **Negorev, D., and G. G. Maul.** 2001. Cellular proteins localized at and interacting within ND10/PML nuclear bodies/PODs suggest functions of a nuclear depot. Oncogene **20:**7234–7242.
55. **Novoa, I., Y. Zhang, H. Zeng, R. Jungreis, H. P. Harding, and D. Ron.** 2003. Stress-induced gene expression requires programmed recovery from translational repression. EMBO J. **22:**1180–1187.
56. **Oda, Y., T. Okada, H. Yoshida, R. J. Kaufman, K. Nagata, and K. Mori.** 2006. Derlin-2 and Derlin-3 are regulated by the mammalian unfolded protein response and are required for ER-associated degradation. J. Cell Biol. **172:**383–393.
57. **Omori, Y., J. Imai, Y. Suzuki, S. Watanabe, A. Tanigami, and S. Sugano.** 2002. OASIS is a transcriptional activator of CREB/ATF family with a transmembrane domain. Biochem. Biophys. Res. Commun. **293:**470–477.
58. **Omori, Y., J. Imai, M. Watanabe, T. Komatsu, Y. Suzuki, K. Kataoka, S. Watanabe, A. Tanigami, and S. Sugano.** 2001. CREB-H: a novel mammalian transcription factor belonging to the CREB/ATF family and functioning via the box-B element with a liver-specific expression. Nucleic Acids Res. **29:** 2154–2162.
59. **Patil, C., and P. Walter.** 2001. Intracellular signaling from the endoplasmic reticulum to the nucleus: the unfolded protein response in yeast and mammals. Curr. Opin. Cell Biol. **13:**349–355.
60. **Plemper, R. K., and D. H. Wolf.** 1999. Retrograde protein translocation: ERADication of secretory proteins in health and disease. Trends Biochem. Sci. **24:**266–270.
61. **Qi, H., C. Fillion, Y. Labrie, J. Grenier, A. Fournier, L. Berger, M. El-Alfy, and C. Labrie.** 2002. AIbZIP, a novel bZIP gene located on chromosome 1q21.3 that is highly expressed in prostate tumors and of which the expression is up-regulated by androgens in LNCaP human prostate cancer cells. Cancer Res. **62:**721–733.
62. **Raggo, C., N. Rapin, J. Stirling, P. Gobeil, E. Smith-Windsor, P. O'Hare, and V. Misra.** 2002. Luman, the cellular counterpart of herpes simplex virus VP16, is processed by regulated intramembrane proteolysis. Mol. Cell. Biol. **22:**5639–5649.
63. **Rao, R. V., A. Peel, A. Logvinova, G. del Rio, E. Hermel, T. Yokota, P. C. Goldsmith, L. M. Ellerby, H. M. Ellerby, and D. E. Bredesen.** 2002. Coupling endoplasmic reticulum stress to the cell death program: role of the ER chaperone GRP78. FEBS Lett. **514:**122–128.
64. **Reddy, R. K., C. Mao, P. Baumeister, R. C. Austin, R. J. Kaufman, and A. S. Lee.** 2003. Endoplasmic reticulum chaperone protein GRP78 protects cells from apoptosis induced by topoisomerase inhibitors: role of ATP binding site in suppression of caspase-7 activation. J. Biol. Chem. **278:**20915–20924.
65. **Roy, B., and A. S. Lee.** 1999. The mammalian endoplasmic reticulum stress response element consists of an evolutionarily conserved tripartite structure and interacts with a novel stress-inducible complex. Nucleic Acids Res. **27:**1437–1443.
66. **Scheuner, D., B. Song, E. McEwen, C. Liu, R. Laybutt, P. Gillespie, T. Saunders, S. Bonner-Weir, and R. J. Kaufman.** 2001. Translational control is required for the unfolded protein response and in vivo glucose homeostasis. Mol. Cell **7:**1165–1176.
67. **Schroder, M., and R. J. Kaufman.** 2005. The mammalian unfolded protein response. Annu. Rev. Biochem. **74:**739–789.
68. **Shen, J., X. Chen, L. Hendershot, and R. Prywes.** 2002. ER stress regulation of ATF6 localization by dissociation of BiP/GRP78 binding and unmasking of Golgi localization signals. Dev. Cell **3:**99–111.
69. **Shen, X., R. E. Ellis, K. Lee, C. Y. Liu, K. Yang, A. Solomon, H. Yoshida, R. Morimoto, D. M. Kurnit, K. Mori, and R. J. Kaufman.** 2001. Complementary signaling pathways regulate the unfolded protein response and are required for *C. elegans* development. Cell **107:**893–903.
70. **Sifers, R. N.** 2003. Cell biology. Protein degradation unlocked. Science **299:** 1330–1331.
71. **Stelzer, G., and J. Don.** 2002. Atce1: a novel mouse cyclic adenosine 3′,5′-monophosphate-responsive element-binding protein-like gene exclusively expressed in postmeiotic spermatids. Endocrinology **143:**1578–1588.
72. **Stirling, J., and P. O'Hare.** 2006. CREB4, a transmembrane bZip transcription factor and potential new substrate for regulation and cleavage by S1P. Mol. Biol. Cell **17:**413–426.
73. **Storlazzi, C. T., F. Mertens, A. Nascimento, M. Isaksson, J. Wejde, O. Brosjo, N. Mandahl, and I. Panagopoulos.** 2003. Fusion of the FUS and BBF2H7 genes in low grade fibromyxoid sarcoma. Hum. Mol. Genet. **12:** 2349–2358.
74. **Strausberg, R. L., E. A. Feingold, L. H. Grouse, J. G. Derge, R. D. Klausner, F. S. Collins, L. Wagner, C. M. Shenmen, G. D. Schuler, S. F. Altschul, B. Zeeberg, K. H. Buetow, C. F. Schaefer, N. K. Bhat, R. F. Hopkins, H. Jordan, T. Moore, S. I. Max, J. Wang, F. Hsieh, L. Diatchenko, K. Marusina, A. A. Farmer, G. M. Rubin, L. Hong, M. Stapleton, M. B. Soares, M. F. Bonaldo, T. L. Casavant, T. E. Scheetz, M. J. Brownstein, T. B. Usdin, S. Toshiyuki, P. Carninci, C. Prange, S. S. Raha, N. A. Loquellano, G. J. Peters, R. D. Abramson, S. J. Mullahy, S. A. Bosak, P. J. McEwan, K. J. McKernan, J. A. Malek, P. H. Gunaratne, S. Richards, K. C. Worley, S. Hale, A. M. Garcia, L. J. Gay, S. W. Hulyk, D. K. Villalon, D. M. Muzny, E. J. Sodergren, X. Lu,**

R. A. Gibbs, J. Fahey, E. Helton, M. Ketteman, A. Madan, S. Rodrigues, A. Sanchez, M. Whiting, A. C. Young, Y. Shevchenko, G. G. Bouffard, R. W. Blakesley, J. W. Touchman, E. D. Green, M. C. Dickson, A. C. Rodriguez, J. Grimwood, J. Schmutz, R. M. Myers, Y. S. Butterfield, M. I. Krzywinski, U. Skalska, D. E. Smailus, A. Schnerch, J. E. Schein, S. J. Jones, and M. A. Marra. 2002. Generation and initial analysis of more than 15,000 full-length human and mouse cDNA sequences. Proc. Natl. Acad. Sci. USA **99:**16899–16903.

75. **Thuerauf, D. J., M. Marcinko, P. J. Belmont, and C. C. Glembotski.** 2007. Effects of the isoform-specific characteristics of ATF6α and ATF6β on endoplasmic reticulum stress response gene expression and cell viability. J. Biol. Chem. **282:**22865–22878.
76. **Thuerauf, D. J., L. Morrison, and C. C. Glembotski.** 2004. Opposing roles for ATF6α and ATF6β in endoplasmic reticulum stress response gene induction. J. Biol. Chem. **279:**21078–21084.
77. **Tyagi, S., A. L. Chabes, J. Wysocka, and W. Herr.** 2007. E2F activation of S phase promoters via association with HCF-1 and the MLL family of histone H3K4 methyltransferases. Mol. Cell **27:**107–119.
78. **Urano, F., X. Wang, A. Bertolotti, Y. Zhang, P. Chung, H. P. Harding, and D. Ron.** 2000. Coupling of stress in the ER to activation of JNK protein kinases by transmembrane protein kinase IRE1. Science **287:**664–666.
79. **van Laar, T., T. Schouten, E. Hoogervorst, M. van Eck, A. J. van der Eb, and C. Terleth.** 2000. The novel MMS-inducible gene Mif1/KIAA0025 is a target of the unfolded protein response pathway. FEBS Lett. **469:**123–131.
80. **Vattem, K. M., and R. C. Wek.** 2004. Reinitiation involving upstream ORFs regulates ATF4 mRNA translation in mammalian cells. Proc. Natl. Acad. Sci. USA **101:**11269–11274.
81. **Voegel, J. J., M. J. Heine, C. Zechel, P. Chambon, and H. Gronemeyer.** 1996. TIF2, a 160 kDa transcriptional mediator for the ligand-dependent activation function AF-2 of nuclear receptors. EMBO J. **15:**3667–3675.
82. **Wang, Y., J. Shen, N. Arenzana, W. Tirasophon, R. J. Kaufman, and R. Prywes.** 2000. Activation of ATF6 and an ATF6 DNA binding site by the endoplasmic reticulum stress response. J. Biol. Chem. **275:**27013–27020.
83. **Wilson, A. C., K. LaMarco, M. G. Peterson, and W. Herr.** 1993. The VP16 accessory protein HCF is a family of polypeptides processed from a large precursor protein. Cell **74:**115–125.
84. **Wu, J., and R. J. Kaufman.** 2006. From acute ER stress to physiological roles of the unfolded protein response. Cell Death Differ. **13:**374–384.
85. **Wu, J., D. T. Rutkowski, M. Dubois, J. Swathirajan, T. Saunders, J. Wang, B. Song, G. D. Yau, and R. J. Kaufman.** 2007. ATF6α optimizes long-term endoplasmic reticulum function to protect cells from chronic stress. Dev. Cell **13:**351–364.
86. **Yamamoto, K., T. Sato, T. Matsui, M. Sato, T. Okada, H. Yoshida, A. Harada, and K. Mori.** 2007. Transcriptional induction of mammalian ER quality control proteins is mediated by single or combined action of ATF6α and XBP1. Dev. Cell **13:**365–376.
87. **Ye, J., R. B. Rawson, R. Komuro, X. Chen, U. P. Dave, R. Prywes, M. S. Brown, and J. L. Goldstein.** 2000. ER stress induces cleavage of membrane-bound ATF6 by the same proteases that process SREBPs. Mol. Cell **6:**1355–1364.
88. **Yoshida, H.** 2007. ER stress and diseases. FEBS J. **274:**630–658.
89. **Yoshida, H., K. Haze, H. Yanagi, T. Yura, and K. Mori.** 1998. Identification of the cis-acting endoplasmic reticulum stress response element responsible for transcriptional induction of mammalian glucose-regulated proteins. Involvement of basic leucine zipper transcription factors. J. Biol. Chem. **273:**33741–33749.
90. **Yoshida, H., T. Matsui, N. Hosokawa, R. J. Kaufman, K. Nagata, and K. Mori.** 2003. A time-dependent phase shift in the mammalian unfolded protein response. Dev. Cell **4:**265–271.
91. **Yoshida, H., T. Matsui, A. Yamamoto, T. Okada, and K. Mori.** 2001. XBP1 mRNA is induced by ATF6 and spliced by IRE1 in response to ER stress to produce a highly active transcription factor. Cell **107:**881–891.
92. **Yoshida, H., T. Okada, K. Haze, H. Yanagi, T. Yura, M. Negishi, and K. Mori.** 2000. ATF6 activated by proteolysis binds in the presence of NF-Y (CBF) directly to the *cis*-acting element responsible for the mammalian unfolded protein response. Mol. Cell. Biol. **20:**6755–6767.
93. **Yoshida, H., T. Okada, K. Haze, H. Yanagi, T. Yura, M. Negishi, and K. Mori.** 2001. Endoplasmic reticulum stress-induced formation of transcription factor complex ERSF including NF-Y (CBF) and activating transcription factors 6α and 6β that activates the mammalian unfolded protein response. Mol. Cell. Biol. **21:**1239–1248.
94. **Yoshida, H., M. Oku, M. Suzuki, and K. Mori.** 2006. pXBP1(U) encoded in XBP1 pre-mRNA negatively regulates unfolded protein response activator pXBP1(S) in mammalian ER stress response. J. Cell Biol. **172:**565–575.
95. **Zilliacus, J., E. Holter, H. Wakui, H. Tazawa, E. Treuter, and J. A. Gustafsson.** 2001. Regulation of glucocorticoid receptor activity by 14-3-3-dependent intracellular relocalization of the corepressor RIP140. Mol. Endocrinol. **15:**501–511.
96. **Zimber, A., Q. D. Nguyen, and C. Gespach.** 2004. Nuclear bodies and compartments: functional roles and cellular signalling in health and disease. Cell. Signal. **16:**1085–1104.